

Electroweak two-loop corrections to the M_W - M_Z mass correlation in the Standard Model

A. FREITAS^{1*}, W. HOLLIK^{2,3}, W. WALTER², AND G. WEIGLEIN^{4†}

¹ *DESY Theorie, Notkestr. 85, D-22603 Hamburg, Germany*

² *Institut für Theoretische Physik, Universität Karlsruhe,
D-76128 Karlsruhe, Germany*

³ *Max-Planck-Institut für Physik, Föhringer Ring 6, D-80805 München, Germany*

⁴ *IPPP, University of Durham, Durham DH1 3LE, United Kingdom*

Abstract

Recently exact results for the complete fermionic two-loop contributions to the prediction for the W-boson mass from muon decay in the electroweak Standard Model have been published [1]. This paper illustrates the techniques that have been applied for this calculation, in particular the renormalisation procedure and the treatment of IR-divergent QED contributions. Numerical results are presented in terms of simple parametrisation formulae and compared in detail with a previous result of an expansion up to next-to-leading order in the top-quark mass. An estimate of the remaining theoretical uncertainties of the M_W -prediction from unknown higher-order corrections is given. For the bosonic two-loop corrections a partial result is presented, yielding the Higgs-mass dependence of these contributions.

*email: Ayres.Freitas@desy.de

†email: Georg.Weiglein@durham.ac.uk

1 Introduction

One of the most important quantities for testing the Standard Model (SM) or its extensions is the relation between the massive gauge boson masses, M_W and M_Z , in terms of the Fermi constant, G_μ , and the fine structure constant, α . This relation can be derived from muon decay, where the Fermi constant enters the muon lifetime, τ_μ , via the expression

$$\tau_\mu^{-1} = \frac{G_\mu^2 m_\mu^5}{192\pi^3} F\left(\frac{m_e^2}{m_\mu^2}\right) \left(1 + \frac{3}{5} \frac{m_\mu^2}{M_W^2}\right) (1 + \Delta q), \quad (1)$$

with $F(x) = 1 - 8x - 12x^2 \ln x + 8x^3 - x^4$. By convention, this defining equation is supplemented with the QED corrections within the Fermi Model, Δq . Results for Δq have been available for a long time at the one-loop [2] and, more recently, at the two-loop level [3]. Commonly, tree-level W propagator effects giving rise to the (numerically insignificant) term $3m_\mu^2/(5M_W^2)$ in eq. (1) are also included in the definition of G_μ , although they are not part of the Fermi Model prediction.

Comparing the prediction for the muon lifetime within the SM with eq. (1) yields the relation

$$M_W^2 \left(1 - \frac{M_W^2}{M_Z^2}\right) = \frac{\pi\alpha}{\sqrt{2}G_\mu} (1 + \Delta r), \quad (2)$$

where the radiative corrections are summarised in the quantity Δr [4]. This relation allows a prediction of M_W , to be tested against the experimental result for M_W . The current accuracy of the measurement of the W-boson mass, $M_W^{\text{exp}} = 80.451 \pm 0.033$ GeV [5], will be further improved in the final LEP analysis and Tevatron Run II [6], each with an error of $\delta M_W \approx 30$ MeV. At the LHC, an error of $\delta M_W \approx 15$ MeV can be expected [7], while a high-luminosity linear collider running in a low-energy mode at the W^+W^- threshold could reach a reduction of the experimental error down to $\delta M_W \approx 6$ MeV [8]. This offers the prospect for highly sensitive tests of the electroweak theory [9], provided that the accuracy of the theoretical prediction matches the experimental precision.

The quantum correction Δr has been under extensive theoretical study over the last two decades. The one-loop result [4] involves large fermionic contributions from the shift in the fine structure constant due to light fermions, $\Delta\alpha \propto \log m_f$, and from the leading contribution to the ρ parameter, $\Delta\rho$, which is quadratically dependent on the top-quark mass m_t , resulting from the top-bottom mass splitting [10],

$$\Delta r^{(\alpha)} = \Delta\alpha - \frac{c_W^2}{s_W^2} \Delta\rho + \Delta r_{\text{rem}}(M_H), \quad (3)$$

with $s_W^2 = 1 - M_W^2/M_Z^2$. The remainder part Δr_{rem} contains in particular the dependence on the Higgs-boson mass, M_H .

Beyond the one-loop order, resummations of the leading one-loop contributions $\Delta\alpha$ and $\Delta\rho$ have been derived [11]. They correctly take into account the terms of the form $(\Delta\rho)^2$, $(\Delta\alpha\Delta\rho)$, and $(\Delta\alpha\Delta r_{\text{rem}})$ at the two-loop level and $(\Delta\alpha)^n$ to all orders.

Beyond the two-loop order, complete results for the pure fermion-loop corrections (i.e. contributions containing n fermion loops at n -loop order) are known up to four-loop order [12]. These results also include the contributions arising from resummation of $\Delta\alpha$ and $\Delta\rho$. Recently, the leading three-loop contributions to the ρ parameter of $\mathcal{O}(G_\mu^3 m_t^6)$ and $\mathcal{O}(G_\mu^2 \alpha_s m_t^4)$ have been computed in the limit of vanishing Higgs boson mass [13], but were found to have small impact on the prediction of the W mass.

Higher order QCD corrections to Δr have been calculated at $\mathcal{O}(\alpha\alpha_s)$ [14] and for the top-bottom contributions at $\mathcal{O}(\alpha\alpha_s^2)$ [15]. The $\mathcal{O}(\alpha\alpha_s^2)$ contributions with light quarks in the loops can be derived from the formulae (29) – (31) in [16] and turn out to be completely negligible. First results for the electroweak two-loop contributions have been obtained using asymptotic expansions for large Higgs [17] and top-quark masses [18, 19, 20]. Concerning the expansion in m_t , the formally leading term of $\mathcal{O}(G_\mu^2 m_t^4)$ [18, 19] and the next-to-leading term of $\mathcal{O}(G_\mu^2 m_t^2 M_Z^2)$ [20] were found to be numerically significant for the prediction of the W mass. Since both contributions turned out to be of similar magnitude and of same sign, a more complete calculation of electroweak two-loop corrections to Δr without using expansions is desirable.

As a first step in this direction, exact results have been obtained for the Higgs-mass dependence (e.g. the quantity $M_{W,\text{subtr}}(M_H) \equiv M_W(M_H) - M_W(M_H = 65 \text{ GeV})$) of the fermionic two-loop corrections to the precision observables [21]. They were shown to agree well with the previous results of the top-quark mass expansion [22].

For the bosonic two-loop corrections to Δr , the complete result is not available up to now. However, in Ref. [23] the effect of the bosonic terms up to $\mathcal{O}(\alpha^2)$ on the relation between the $\overline{\text{MS}}$ and on-shell definition of the gauge boson masses has been studied. For this purpose the corresponding two-loop self-energies have been evaluated in the $\overline{\text{MS}}$ -scheme using large-mass expansions.

This paper discusses the exact computation of all fermionic two-loop corrections to Δr which has been presented recently [1]. These include all two-loop diagrams contributing to the muon decay amplitude and containing at least one closed fermion loop (except the pure QED corrections already contained in the Fermi Model result, see eq. (1)). Some typical examples are shown in Fig. 1. No expansion in the top-quark mass or the Higgs boson mass is made, so that the full dependence on m_t and M_H as well as the complete light-fermion contributions at two-loop order are contained. Previously, corrections from light fermions have only been taken into account via resummations of the one-loop light-fermion contribution (the two-loop light-fermion contributions have been calculated within the $\overline{\text{MS}}$ -scheme in Ref. [24]).

The result of [1] has been included in the Standard Model fits and the indirect derivation of constraints on the Higgs boson mass performed by the LEP Electroweak Working Group [5].

As a further step towards a complete two-loop result for Δr , a partial result is presented for the purely bosonic electroweak two-loop corrections which yields the Higgs-mass dependence of these terms.

The paper is organised as follows. Sections 2–4 enlarge on the methods which were employed for the calculation of the fermionic two-loop corrections. While section 2 presents

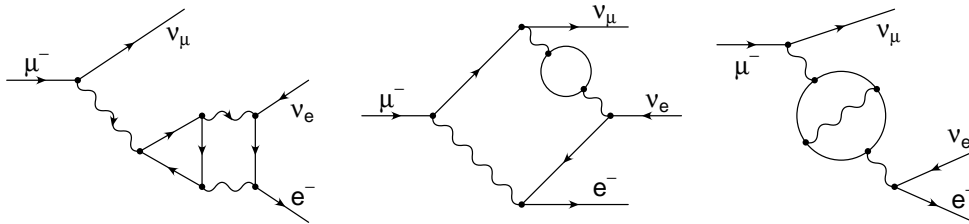


Figure 1: Examples for types of fermionic two-loop diagrams contributing to muon decay.

an overview over the techniques, the renormalisation procedure is explained in section 3 and the extraction of the QED corrections, which are already contained in the Fermi Model, is described in section 4. A discussion of the numerical results and remaining theoretical uncertainties due to unknown higher orders can be found in sections 5 and 6, respectively. In section 7 the Higgs-mass dependence of the bosonic two-loop corrections is studied. Before concluding, an outlook to the situation for future colliders is given in section 8.

2 Outline of the two-loop calculation

This section presents an overview over the main features of the calculation.

Since the definition of the Fermi coupling constant according to eq. (1) contains QED corrections in the Fermi Model summarised in the quantity Δq , the corresponding contributions have to be identified and extracted from the Standard Model computation of muon decay in order to arrive at the quantity Δr . As shown in section 4 below, all IR-divergent loop contributions in our calculation are already contained in Δq , contributing to Δr are IR-finite. As a consequence, after extraction of the Fermi Model contributions, it is possible to neglect the masses and momenta of the external particles, thereby reducing the generic diagrams contributing to the muon-decay amplitude to vacuum diagrams.

For the renormalisation the on-shell scheme is used throughout. It entails, in addition, the evaluation of two-loop two-point functions with non-zero external momentum, which is technically more involved. However, it should be noted that the evaluation of this type of integrals is generally necessary in all renormalisation schemes if the result shall be related to the physical gauge boson masses. The details of the renormalisation procedure are given in section 3.

Since the calculation involves the computation of more than thousand diagrams, it is convenient to employ computer-algebra tools. The generation of diagrams and Feynman amplitudes, including the counterterm contributions, was performed with the package *FeynArts* [25]. The program *TwoCalc* [26] was applied for the algebraic evaluation of these amplitudes, which were reduced, by means of two-loop tensor-integral decompositions, to a set of standard scalar integrals. Throughout the calculation, a general R_ξ gauge was used, and the gauge-parameter independence of the final result was checked algebraically. For the evaluation of the scalar one-loop integrals and the two-loop vacuum integrals we have

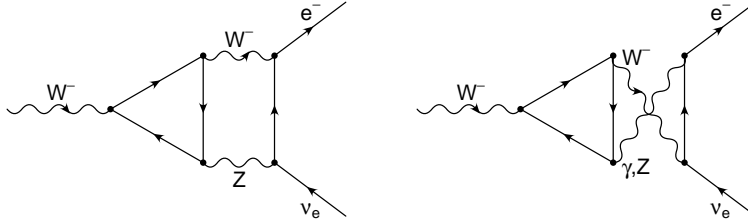


Figure 2: Two-loop vertex diagrams containing a triangle subgraph, which require a careful treatment of γ_5 in D dimensions.

used analytical results as given in Refs. [27, 28], while the two-loop two-point integrals with non-vanishing external momentum have been evaluated numerically using one-dimensional integral representations with elementary functions [29]. These allow a fast and stable calculation of the integrals for general mass configurations.

Since we use Dimensional Regularisation [30, 31] in our calculation, it is necessary to investigate the treatment of the Dirac algebra involving γ_5 . It is known that a naively anti-commuting γ_5 respects all Ward identities of the Standard Model [32]. However, while it can safely be applied for all two-loop two-point contributions (for a discussion, see e.g. Ref. [18]) and most of the two-loop vertex- and box-type diagrams, it would yield an incorrect result for vertex diagrams containing a triangle subgraph (see Fig. 2). This originates from an inconsistent treatment of the trace of γ_5 together with four Dirac matrices, which in four dimensions is given by $\text{Tr} \{ \gamma_5 \gamma^\mu \gamma^\nu \gamma^\rho \gamma^\sigma \} = 4i \epsilon^{\mu\nu\rho\sigma}$, while this trace would vanish when using the naively anti-commuting γ_5 in D dimensions.

A mathematically consistent definition of γ_5 in D dimensions [31, 33] would require the introduction of additional counterterms to restore the Ward identities, which is a very tedious procedure at the two-loop level. For recent discussions on this topic, see Refs. [35, 34].

In order to calculate the class of diagrams in Fig. 2, we have first evaluated the triangle subgraph with a consistent γ_5 according to Refs. [31, 33] (here we made use of the package TRACER [36] for checking). After adding appropriate counterterms to restore the Ward identities, the result differs from the result obtained using a naively anti-commuting γ_5 only in terms proportional to the totally antisymmetric tensor $\epsilon^{\mu\nu\rho\sigma}$, which are finite for $D \rightarrow 4$. Inserting this difference term into the two-loop diagrams, it turns out that the second loop only yields a finite contribution, so that it can be evaluated in four dimensions without further complications. After contraction with the external fermion line in the vertex diagrams, a non-zero contribution to the result for Δr is obtained from this term.

3 On-shell Renormalisation

3.1 One-loop renormalisation

In the on-shell renormalisation scheme the mass parameters and coupling constants are related to physical observables. The gauge bosons of the U(1) and SU(2)_L group, $B_\mu, W_\mu^{1,2,3}$

are conveniently expressed in terms of their mass eigenstates,

$$W_\mu^\pm = \frac{1}{\sqrt{2}} (W_\mu^1 \mp iW_\mu^2), \quad (4)$$

$$\begin{pmatrix} Z_\mu \\ A_\mu \end{pmatrix} = \begin{pmatrix} c_W & s_W \\ -s_W & c_W \end{pmatrix} \begin{pmatrix} W_\mu^3 \\ B_\mu \end{pmatrix}, \quad (5)$$

where W_μ^\pm, Z_μ denote the fields of the massive vector bosons W, Z with masses M_W, M_Z , A_μ represents the massless photon field, and the weak mixing angle enters in the combination

$$c_W = \cos \theta_W = M_W/M_Z, \quad s_W = \sin \theta_W = \sqrt{1 - M_W^2/M_Z^2}. \quad (6)$$

The eigenstates of the Higgs doublet are the physical Higgs field H with mass M_H and the neutral and charged Goldstone bosons χ, ϕ^\pm . We neglect mixing between the fermion generations throughout.

In the following the conventions of [37] are adopted. In our approach all physical fields and masses as well as the electromagnetic coupling e are renormalised:

$$\begin{aligned} e_0 &= Z_e e, \\ M_{W0}^2 &= M_W^2 + \delta M_W^2, & M_{Z0}^2 &= M_Z^2 + \delta M_Z^2, \\ M_{H0}^2 &= M_H^2 + \delta M_H^2, & m_{f0} &= m_f + \delta m_f, \\ W_0^\pm &= (Z^W)^{1/2} W^\pm, & Z_0 &= (Z^{ZZ})^{1/2} Z + \frac{1}{2} \delta Z^{Z\gamma} A, \\ & & A_0 &= \frac{1}{2} \delta Z^{\gamma Z} Z + (Z^{\gamma\gamma})^{1/2} A, \\ H_0 &= (Z^H)^{1/2} H, & f_0^L &= (Z^{fL})^{1/2} f^L \quad (f = e, \nu_e, \dots), \\ & & f_0^R &= (Z^{fR})^{1/2} f^R. \end{aligned} \quad (7)$$

Here the index 0 indicates the bare quantities. The renormalisation constants for the masses, $\delta M_X, \delta m_f$, the fields, $Z^X = 1 + \delta Z^X$, and the charge, $Z_e = 1 + \delta Z_e$, are fixed by on-shell renormalisation conditions.

The physical squared masses M_X^2 are defined as the real part of the poles \mathcal{M}_X^2 of the propagators D^X . The field renormalisation constants are determined by demanding unity residues of the poles. This ensures that all Green's functions are finite and external wave function corrections need not be taken into account. With the index T denoting the transverse part

of the vector boson propagators, the on-shell renormalisation conditions read

$$\begin{aligned}
(D_{\text{T}}^{\text{W}})^{-1}(\mathcal{M}_{\text{W}}^2) &= 0, & \text{Re}\left\{i\frac{\partial}{\partial k^2}(D_{\text{T}}^{\text{W}})^{-1}(k^2)\Big|_{k^2=\mathcal{M}_{\text{W}}^2}\right\} &= -1, \\
(D_{\text{T}}^{\text{ZZ}})^{-1}(\mathcal{M}_{\text{Z}}^2) &= 0, & \text{Re}\left\{i\frac{\partial}{\partial k^2}(D_{\text{T}}^{\text{ZZ}})^{-1}(k^2)\Big|_{k^2=\mathcal{M}_{\text{Z}}^2}\right\} &= -1, \\
(D_{\text{T}}^{\gamma\text{Z}})^{-1}(\mathcal{M}_{\text{Z}}^2) &= 0, \quad (D_{\text{T}}^{\gamma\text{Z}})^{-1}(0) = 0, & \text{Re}\left\{i\frac{\partial}{\partial k^2}(D_{\text{T}}^{\gamma\text{Z}})^{-1}(k^2)\Big|_{k^2=0}\right\} &= -1, \\
(D^{\text{H}})^{-1}(\mathcal{M}_{\text{H}}^2) &= 0, & \text{Re}\left\{i\frac{\partial}{\partial k^2}(D^{\text{H}})^{-1}(k^2)\Big|_{k^2=\mathcal{M}_{\text{H}}^2}\right\} &= 1, \\
(D^f)^{-1}(p)\Big|_{p^2=\mathcal{M}_f^2} &= 0, & \text{Re}\left\{i\frac{\partial}{\partial \not{p}}(D^f)^{-1}(p)\Big|_{p^2=\mathcal{M}_f^2}\right\} &= 1.
\end{aligned} \tag{8}$$

The propagators are related to the one-particle-irreducible two-point functions $\hat{\Gamma}$ by

$$\begin{aligned}
D_{\text{T}}^{\text{W}} &= -(\hat{\Gamma}_{\text{T}}^{\text{W}})^{-1}, & \begin{pmatrix} D_{\text{T}}^{\text{ZZ}} & D_{\text{T}}^{\gamma\text{Z}} \\ D_{\text{T}}^{\gamma\text{Z}} & D_{\text{T}}^{\gamma\gamma} \end{pmatrix} &= -\begin{pmatrix} \hat{\Gamma}_{\text{T}}^{\text{ZZ}} & \hat{\Gamma}_{\text{T}}^{\gamma\text{Z}} \\ \hat{\Gamma}_{\text{T}}^{\gamma\text{Z}} & \hat{\Gamma}_{\text{T}}^{\gamma\gamma} \end{pmatrix}^{-1}, \\
D^{\text{H}} &= -(\hat{\Gamma}^{\text{H}})^{-1}, & &
\end{aligned} \tag{9}$$

$$D^f = -(\hat{\Gamma}^f)^{-1} = -(\not{p}\omega_- \hat{\Gamma}_{\text{L}}^f + \not{p}\omega_+ \hat{\Gamma}_{\text{R}}^f + m_f \hat{\Gamma}_{\text{S}}^f)^{-1}. \tag{10}$$

Here $\hat{\Gamma}_{\text{L,R,S}}^f$ represent the left-/right-handed and scalar component of the fermion two-point functions, respectively. The two-point functions can be separated into a Born contribution and the self-energies,

$$\hat{\Gamma}_{\text{T}}^{ab}(k^2) = i \left[(k^2 - M_a^2) \delta_{ab} + \hat{\Sigma}_{\text{T}}^{ab}(k^2) \right], \tag{11}$$

$$\hat{\Gamma}_{\text{L,R}}^f(p^2) = i \left[1 + \hat{\Sigma}_{\text{L,R}}^f(p^2) \right], \quad \hat{\Gamma}_{\text{S}}^f(p^2) = i \left[-1 + \hat{\Sigma}_{\text{S}}^f(p^2) \right]. \tag{12}$$

The hat indicates renormalised quantities, i. e. $\hat{\Sigma} = \Sigma + \text{counterterms}$.

In addition to the aforementioned renormalisation conditions, one has the freedom to renormalise the Higgs tadpole t . Here the condition

$$t + \delta t = 0 \tag{13}$$

is applied, which requires that all tadpole contributions are exactly cancelled by the counterterms δt , so that no tadpoles need to be taken into account in the actual calculation.

Using the renormalisation conditions eq. (8) one obtains for the renormalisation constants

in eq. (7) at the one-loop level

$$\begin{aligned}
\delta M_W^2 &= \text{Re}\{\Sigma_T^W(M_W^2)\}, & \delta Z^W &= -\text{Re}\{\Sigma_T^{W'}(M_W^2)\}, \\
\delta M_Z^2 &= \text{Re}\{\Sigma_T^{ZZ}(M_Z^2)\}, & \delta Z^{ZZ} &= -\text{Re}\{\Sigma_T^{ZZ'}(M_Z^2)\}, \\
& & \delta Z^{\gamma Z} &= -2 \text{Re}\left\{\frac{\Sigma_T^{\gamma Z}(M_Z^2)}{M_Z^2}\right\}, \\
& & \delta Z^{Z\gamma} &= 2 \frac{\Sigma_T^{\gamma Z}(0)}{M_Z^2}, \\
& & \delta Z^{\gamma\gamma} &= -\Sigma_T^{\gamma\gamma'}(0), \\
\delta M_H^2 &= \text{Re}\{\Sigma^H(M_H^2)\}, & \delta Z^H &= -\text{Re}\{\Sigma^{H'}(M_H^2)\},
\end{aligned} \tag{14}$$

$$\begin{aligned}
\delta m_f &= \frac{m_f}{2} \text{Re}\left\{\Sigma_L^f(m_f^2) + \Sigma_R^f(m_f^2) + 2\Sigma_S^f(m_f^2)\right\}, \\
\delta Z^{fL} &= -\text{Re}\{\Sigma_L^f(m_f^2)\} - m_f^2 \text{Re}\left\{\Sigma_L^{f'}(m_f^2) + \Sigma_R^{f'}(m_f^2) + 2\Sigma_S^{f'}(m_f^2)\right\}, \\
\delta Z^{fR} &= -\text{Re}\{\Sigma_R^f(m_f^2)\} - m_f^2 \text{Re}\left\{\Sigma_L^{f'}(m_f^2) + \Sigma_R^{f'}(m_f^2) + 2\Sigma_S^{f'}(m_f^2)\right\},
\end{aligned} \tag{15}$$

with $\Sigma'(k^2)$ indicating the derivative of the self-energy with respect to k^2 .

For the charge renormalisation an additional condition is required. Usually it is fixed by demanding that the electric charge e coincides with the coupling of the electromagnetic vertex in the Thomson limit,

$$\bar{u}(p) \hat{\Gamma}_\mu^{ee\gamma}(p, p) u(p) \Big|_{p^2=m_e^2} = ie\bar{u}(p)\gamma_\mu u(p). \tag{16}$$

Employing the U(1) Ward identity this yields at one-loop order

$$\delta Z_e = -\frac{1}{2}\delta Z^{\gamma\gamma} - \frac{s_W}{2c_W}\delta Z^{Z\gamma}. \tag{17}$$

The weak mixing angle is a derived quantity, expressed in terms of the gauge boson masses, see eq. (6). Thus the renormalisation of M_W, M_Z also determines the counterterm δs_W for s_W [4]. At one-loop order one obtains

$$\frac{\delta s_W}{s_W} = \frac{c_W^2}{2s_W^2} \left[\frac{\delta M_Z^2}{M_Z^2} - \frac{\delta M_W^2}{M_W^2} \right]. \tag{18}$$

From two-loop order on, a one-loop sub-renormalisation is necessary for the Faddeev-Popov ghost sector, which is associated with the gauge-fixing part. It is possible to keep the gauge-fixing part invariant under renormalisation. For technical convenience, we arrange for this by a renormalisation of the gauge parameters in such a way that it precisely cancels the renormalisation of the parameters and fields in the gauge-fixing Lagrangian.¹ To this end,

¹In another approach to avoid counterterms emerging from the gauge-fixing sector, the gauge-fixing part could alternatively be added to the Lagrangian only after renormalisation. In this case the counterterms to the ghost sector arise only from the renormalisation of the gauge transformations and not from the gauge-fixing functions F^V .

we start with the following, rather general form of the bare gauge-fixing term:

$$\mathcal{L}_{\text{gf}} = -\frac{1}{2}\left((F^\gamma)^2 + (F^Z)^2 + F^+F^- + F^-F^+\right), \quad (19)$$

$$F^\gamma = (\xi_1^\gamma)^{-\frac{1}{2}}\partial_\mu A^\mu + \frac{\xi^{\gamma Z}}{2}\partial_\mu Z^\mu, \quad (20)$$

$$F^Z = (\xi_1^Z)^{-\frac{1}{2}}\partial_\mu Z^\mu + \frac{\xi^{Z\gamma}}{2}\partial_\mu A^\mu - (\xi_2^Z)^{\frac{1}{2}}M_Z\chi, \quad (21)$$

$$F^\pm = (\xi_1^W)^{-\frac{1}{2}}\partial_\mu W^{\pm\mu} \mp i(\xi_2^W)^{\frac{1}{2}}M_W\phi^\pm, \quad (22)$$

allowing two different bare gauge parameters for both W and Z, $\xi_1^{W,Z}$ and $\xi_2^{W,Z}$, and also mixing gauge parameters, $\xi^{\gamma Z}$ and $\xi^{Z\gamma}$. The renormalised parameters shall comply with the R_ξ gauge, providing one free gauge parameter for each gauge boson, ξ^γ, ξ^Z, ξ^W . With the following renormalisation prescription

$$\begin{pmatrix} (\xi^\gamma)^{-\frac{1}{2}} & 0 \\ 0 & (\xi^Z)^{-\frac{1}{2}} \end{pmatrix} = \begin{pmatrix} (\xi_1^\gamma)^{-\frac{1}{2}} & \frac{1}{2}\xi^{\gamma Z} \\ \frac{1}{2}\xi^{Z\gamma} & (\xi_1^Z)^{-\frac{1}{2}} \end{pmatrix} \begin{pmatrix} (Z^{\gamma\gamma})^{\frac{1}{2}} & \frac{1}{2}\delta Z^{\gamma Z} \\ \frac{1}{2}\delta Z^{Z\gamma} & (Z^{ZZ})^{\frac{1}{2}} \end{pmatrix}, \quad (23)$$

$$\xi^Z = \xi_2^Z \frac{M_Z^2 + \delta M_Z^2}{M_Z^2} Z^\chi, \quad (24)$$

$$\xi^W = \frac{1}{Z^W} \xi_1^W \quad \xi^W = \xi_2^W \frac{M_W^2 + \delta M_W^2}{M_W^2} Z^\phi \quad (25)$$

no counterterm contributions arise from the gauge-fixing sector. Here we have allowed for field renormalisation constants $\delta Z^\chi, \delta Z^\phi$ of the unphysical scalars χ, ϕ^\pm as well. Starting at the two-loop level, counterterm contributions from the ghost sector have to be taken into account in the calculation of physical amplitudes. They follow from the variation of the gauge-fixing terms F^a under infinitesimal gauge transformations, $\delta\theta^b, b = \gamma, Z, \pm$,

$$\mathcal{L}_{\text{FP}} = \sum_{a,b=\gamma,Z,\pm} \bar{u}^a \frac{\delta F^a}{\delta\theta^b} u^b = \int d^4y \sum_{a,b} \bar{u}^a(x) \frac{\delta F^a(x)}{\delta\theta^b(y)} u^b(y). \quad (26)$$

These contributions can be derived from the action of the gauge transformations on the gauge and Goldstone fields as follows,

$$\begin{aligned} A_\mu &\rightarrow A_\mu + \partial_\mu \delta\theta^\gamma + ie(W_\mu^+ \delta\theta^- - W_\mu^- \delta\theta^+), \\ Z_\mu &\rightarrow Z_\mu + \partial_\mu \delta\theta^Z - ie \frac{c_W}{s_W} (W_\mu^+ \delta\theta^- - W_\mu^- \delta\theta^+), \\ W_\mu^\pm &\rightarrow W_\mu^\pm + \partial_\mu \delta\theta^\pm \mp ie \left(W_\mu^\pm \delta\theta^\gamma - \frac{c_W}{s_W} W_\mu^\pm \delta\theta^Z - A_\mu \delta\theta^\pm + \frac{c_W}{s_W} Z_\mu \delta\theta^\pm \right), \\ \chi &\rightarrow \chi - \left(M_Z + \frac{e}{2s_W c_W} H \right) \delta\theta^Z + \frac{e}{2s_W} (\phi^+ \delta\theta^- + \phi^- \delta\theta^+), \\ \phi^\pm &\rightarrow \phi^\pm \mp ie \phi^\pm \delta\theta^\gamma \mp ie \frac{s_W^2 - c_W^2}{2c_W s_W} \phi^\pm \delta\theta^Z \pm \left(iM_W + \frac{ie}{2s_W} H \mp \frac{e}{2s_W} \chi \right) \delta\theta^\pm. \end{aligned} \quad (27)$$

We have derived all the counterterms arising from the ghost sector (extending the results of Refs. [38, 39] to a general R_ξ gauge) and implemented them into the program *FeynArts*. In this way we could verify the finiteness of individual (gauge-parameter-dependent) building blocks (e.g. the W- and the Z-boson self-energy) as a further check of the calculation. The explicit Feynman rules of the ghost sector including counterterms can be found in the appendix.

3.2 Two-loop counterterms

In the $\mathcal{O}(\alpha^2)$ calculation of the muon decay, two-loop counterterms arise for the transverse W propagator and the charged current vertex:

$$\left[\text{wavy line with } \otimes \text{ in the middle} \right]_{\text{T}} = \delta Z_{(2)}^{\text{W}}(k^2 - M_{\text{W}}^2) - \delta M_{\text{W},(2)}^2 - \delta Z_{(1)}^{\text{W}} \delta M_{\text{W},(1)}^2, \quad (28)$$

$$\begin{aligned} \left[\text{W}^* \text{ line with } \otimes \text{ in the middle, } \nu_e \text{ and } e \text{ lines} \right] &= i \frac{e}{\sqrt{2}s_{\text{W}}} \gamma_\mu \omega_- \left[\delta Z_{e(2)} - \frac{\delta s_{\text{W}}}{s_{\text{W}}} + \frac{1}{2} \left(\delta Z_{(2)}^{e\text{L}} + \delta Z_{(2)}^{\text{W}} + \delta Z_{(2)}^{\nu\text{L}} \right) \right. \\ &\quad \left. + (1\text{-loop renormalisation constants}) \right]. \end{aligned} \quad (29)$$

The numbers in parentheses indicate the loop order. Throughout this paper, the two-loop contributions always include the subloop renormalisation.

Concerning the mass renormalisation of unstable particles, from two-loop order on it makes a difference whether the mass is defined according to the real part of the complex pole of the S matrix,

$$\mathcal{M}^2 = \overline{M}^2 - i\overline{M}\overline{\Gamma}, \quad (30)$$

or according to the pole of the real part of the propagator. In eq. (30) \mathcal{M} denotes the complex pole of the S matrix as specified by the renormalisation conditions in eq. (8). \overline{M} , $\overline{\Gamma}$ are then interpreted as the corresponding mass and width of the unstable particle. For the real pole, on the other hand, we use the symbol \widetilde{M} . It is determined by

$$\text{Re}\{(D_{\text{T}})^{-1}(\widetilde{M}^2)\} = 0. \quad (31)$$

In the context of the present calculation, these considerations are relevant for the renormalisation of the gauge-boson masses, M_{W} and M_{Z} . The two-loop mass counterterms according to the definition of the mass as the real part of the complex pole are obtained from eq. (8),

$$\delta \overline{M}_{\text{W},(2)}^2 = \text{Re} \left\{ \Sigma_{\text{T},(2)}^{\text{W}}(M_{\text{W}}^2) \right\} - \delta M_{\text{W},(1)}^2 \delta Z_{(1)}^{\text{W}} + \text{Im} \left\{ \Sigma_{\text{T},(1)}^{\text{W}'}(M_{\text{W}}^2) \right\} \text{Im} \left\{ \Sigma_{\text{T},(1)}^{\text{W}}(M_{\text{W}}^2) \right\}, \quad (32)$$

$$\begin{aligned} \delta \overline{M}_{\text{Z},(2)}^2 &= \text{Re} \left\{ \Sigma_{\text{T},(2)}^{\text{ZZ}}(M_{\text{Z}}^2) \right\} - \delta M_{\text{Z},(1)}^2 \delta Z_{(1)}^{\text{ZZ}} + \frac{M_{\text{Z}}^2}{4} \left(\delta Z_{(1)}^{\gamma\text{Z}} \right)^2 + \frac{\left(\text{Im} \left\{ \Sigma_{\text{T},(1)}^{\gamma\text{Z}}(M_{\text{Z}}^2) \right\} \right)^2}{M_{\text{Z}}^2} \\ &\quad + \text{Im} \left\{ \Sigma_{\text{T},(1)}^{\text{ZZ}'}(M_{\text{Z}}^2) \right\} \text{Im} \left\{ \Sigma_{\text{T},(1)}^{\text{ZZ}}(M_{\text{Z}}^2) \right\}. \end{aligned} \quad (33)$$

When compared with the mass counterterms according to the real-pole definition, $\delta\widetilde{M}_{\text{W},(2)}^2$ and $\delta\widetilde{M}_{\text{Z},(2)}^2$, there remains a finite difference,

$$\delta\overline{M}_{\text{W},(2)}^2 = \delta\widetilde{M}_{\text{W},(2)}^2 + \text{Im} \left\{ \Sigma_{\text{T},(1)}^{\text{W}'/}(M_{\text{W}}^2) \right\} \text{Im} \left\{ \Sigma_{\text{T},(1)}^{\text{W}}(M_{\text{W}}^2) \right\}, \quad (34)$$

$$\delta\overline{M}_{\text{Z},(2)}^2 = \delta\widetilde{M}_{\text{Z},(2)}^2 + \text{Im} \left\{ \Sigma_{\text{T},(1)}^{\text{ZZ}'/}(M_{\text{Z}}^2) \right\} \text{Im} \left\{ \Sigma_{\text{T},(1)}^{\text{ZZ}}(M_{\text{Z}}^2) \right\}. \quad (35)$$

It can easily be checked by direct computation that the difference terms in eqs. (34), (35) are gauge-parameter-dependent, thus showing that at least one of the two prescriptions leads to a gauge-dependent mass definition. The problem of a proper definition of unstable particles in gauge theories has already been addressed several times in the literature [40]. However, the present work, for the first time, involves an explicit calculation of a physical process which is sensitive to the gauge-parameter dependent difference between the two mass renormalisation methods. In the previous results for M_{W} , incorporating terms up to $\mathcal{O}(G_{\mu}^2 m_{\text{t}}^2 M_{\text{Z}}^2)$ [20] and M_{H} -dependent fermionic terms [21], the contribution $\text{Im} \left\{ \Sigma'_{\text{T},(1)}(M^2) \right\} \text{Im} \left\{ \Sigma_{\text{T},(1)}(M^2) \right\}$ was zero, making thus a strict distinction between the two mass definitions unnecessary at the considered order.

Using a general R_{ξ} gauge, we can test the two mass renormalisation prescriptions in our result by regarding the two-loop counterterms to physical observables, which should be gauge-parameter independent. In particular, we only find an invariant result for the counterterm to the weak mixing angle, $\delta s_{\text{W},(2)}$, with the definition of the gauge-boson masses according to the complex pole.

In order to verify the gauge-parameter independence of the mass counterterms $\delta M_{\text{W},(2)}^2$, $\delta M_{\text{Z},(2)}^2$ one needs an appropriate treatment of the Higgs tadpole diagrams, which do not contribute to physical observables. Alternatively to eq. (13), one can include all Higgs tadpole diagrams in the calculation by demanding the tadpole counterterm to be zero, $\delta t = 0$. Technically, this corresponds to the inclusion of all tadpole diagrams not only in the two-loop self-energies, but also in the subloop renormalisation. In this case, also the mass counterterms themselves are gauge-parameter independent when using the mass definition via the complex pole.

These results confirm the expectations from S-matrix theory that the complex pole is a gauge-invariant quantity [40].

We have thus adopted the complex-pole definition as given in eq. (32) and eq. (33). Using this mass definition and expanding the gauge boson propagator around its pole

$$(D_{\text{T}})^{-1}(q^2) = (D_{\text{T}})^{-1}(\mathcal{M}^2) + (q^2 - \mathcal{M}^2) \left. \frac{\partial}{\partial k^2} (D_{\text{T}})^{-1}(k^2) \right|_{k^2=\mathcal{M}^2} + \mathcal{O}((q^2 - \mathcal{M}^2)^2) \quad (36)$$

one obtains with the renormalisation conditions eq. (8)

$$D_{\text{T}}(q^2) = \frac{-i \text{const.}}{q^2 - \overline{M}^2 + i \overline{M} \overline{\Gamma}} + \text{non-resonant terms}, \quad (37)$$

which corresponds to a Breit–Wigner parametrisation of the resonance line shape with a constant decay width.

Experimentally the gauge-boson masses are determined using a Breit–Wigner function with a running (energy-dependent) width,

$$D_T(q^2) \propto \frac{-i}{q^2 - M^2 + i q^2 \Gamma/M}. \quad (38)$$

As a consequence of the different Breit–Wigner parametrisations, there is a numerical difference between the experimental mass parameters (denoted as M_W , M_Z henceforth) and the mass parameters in our calculation, \overline{M}_W , \overline{M}_Z . The shift between these parameters is given by [42] $M_{W,Z} = \overline{M}_{W,Z} + \Gamma_{W,Z}^2/(2M_{W,Z})$. Since M_W and M_Z enter on a different footing in our computation — M_Z is an experimental input parameter, while M_W is calculated — in order to evaluate the mass shifts we use the experimental value for the Z-boson width, $\Gamma_Z = 2.944 \pm 0.0024$ GeV [5], and the theoretical value for the W-boson width, which is given by $\Gamma_W = 3G_\mu M_W^3/(2\sqrt{2}\pi)(1 + 2\alpha_s/(3\pi))$ in sufficiently good approximation. This results in $M_Z \approx \overline{M}_Z + 34.1$ MeV and in the mass shifts $M_W \approx \overline{M}_W + 27.4$ MeV and $M_W \approx \overline{M}_W + 27.0$ MeV for $M_W = 80.4$ GeV and $M_W = 80.2$ GeV, respectively.²

For an extension of the renormalisation formalism for unstable particles to higher loop orders and to the field renormalisation of unstable particles, see Refs. [43]. However, in a physical process with particles in the initial and final state whose mass can be neglected, a treatment of complex poles is only necessary for internal particles. Since the field renormalisation of internal particles does not contribute to the physical result, it is not necessary to examine this issue for our purposes.

The two-loop charge renormalisation constant follows from the condition eq. (16). With the help of the U(1) Ward identity the electromagnetic vertex can be related to photonic two-point functions, thus resulting in the following relation between the renormalisation constants, which is valid in all orders of perturbation theory [39]:

$$Z_e \left((Z^{\gamma\gamma})^{1/2} + \frac{s_W + \delta s_W}{c_W + \delta c_W} \frac{\delta Z^{Z\gamma}}{2} \right) = 1. \quad (39)$$

Expansion up to $\mathcal{O}(\alpha^2)$ yields

$$\delta Z_{e(2)} = -\frac{1}{2}\delta Z_{(2)}^{\gamma\gamma} - \frac{s_W}{2c_W}\delta Z_{(2)}^{Z\gamma} + (\delta Z_{e(1)})^2 + \frac{1}{8}(\delta Z_{(1)}^{\gamma\gamma})^2 - \frac{1}{2c_W^3}\delta Z_{(1)}^{Z\gamma}\delta s_{W(1)}. \quad (40)$$

Furthermore the two-loop field renormalisation constants for the external leptons are needed in eq. (29). These can be easily obtained in the limit of vanishing masses and momenta of the external fermions, yielding

$$\delta Z_{(2)}^{fL} = -\Sigma_{(2)}^{fL}(m_f^2 = 0). \quad (41)$$

²The difference in Γ_W according to the way it is calculated, through the tree-level result parametrised with α , or the improved Born result parametrised with G_μ , or the improved Born result including QCD corrections (which is the one we used), is formally of higher order (i.e. beyond $\mathcal{O}(\alpha^2)$) in the calculation of M_W . Its numerical effect is nevertheless not completely negligible; it changes the shift in M_W by about -2.9 MeV if the tree-level result for Γ_W parametrised with α is used and by about -1.4 MeV if the G_μ parametrisation of the Born width (without QCD corrections) is employed.

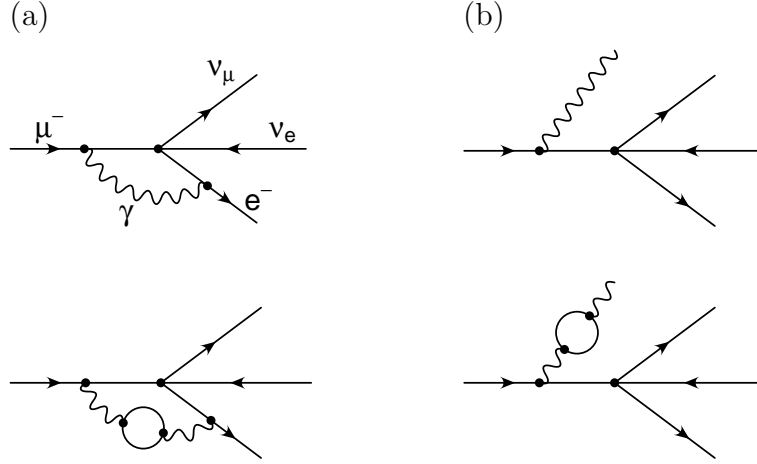


Figure 3: Virtual (a) and real (b) QED corrections to muon decay in the Fermi Model.

4 Extraction of Fermi Model QED contributions

In the evaluation of Δr , the IR-divergent QED corrections that are already contained in the Fermi Model QED factor have to be extracted. For the two-loop calculation presented here, the corresponding Fermi Model contributions consist of virtual and real photonic corrections of order $\mathcal{O}(\alpha)$ and of order $\mathcal{O}(\alpha^2)$ with one closed fermion loop, see Fig. 3, where it is understood that all lepton and quark flavours can appear in the loop. Denoting the virtual corrections to the Fermi Model by Δq_V and the real corrections by Δq_R , this reads

$$|\mathcal{M}_{\text{Fermi}}|^2 = |\mathcal{M}_{\text{Born}}|^2 (1 + \Delta q) = |\mathcal{M}_{\text{Born}}|^2 \left(1 + \Delta q_V^{(\alpha)} + \Delta q_R^{(\alpha)} + \Delta q_V^{(\alpha^2)} + \Delta q_R^{(\alpha^2)} \right). \quad (42)$$

The calculation of the virtual corrections to muon decay in the full Standard Model involves box-type diagrams with IR divergences. In the following, all Standard Model contributions involving photons in the loop are encompassed by the quantity $\Delta\tau$. The one-loop QED corrections $\Delta\tau_V^{(\alpha)}$ originate from the diagram given in Fig. 4 (a). At two-loop order one can distinguish between corrections with only electromagnetic couplings in addition to the tree-level couplings, $\Delta\tau_{V,\text{em}}^{(\alpha^2)}$, see Fig. 4 (b), and corrections with additional QED and non-QED couplings, $\Delta\tau_{V,\text{em/weak}}^{(\alpha^2)}$, see Fig. 4 (c). Here it is always understood that the two-loop corrections involve one closed fermion loop. By performing a tensor integral decomposition of these classes of diagrams one observes that they can be expressed in terms of the virtual corrections in the Fermi Model and an IR-finite remainder Δr_{fr} ,

$$\Delta\tau_V^{(\alpha)} = \Delta q_V^{(\alpha)} + 2 \Delta r_{\text{fr}}^{(\alpha)} \quad (43)$$

$$\Delta\tau_{V,\text{em}}^{(\alpha^2)} = \Delta q_V^{(\alpha^2)} + 2 \Delta r_{\text{fr},1}^{(\alpha^2)} \quad (44)$$

$$\Delta\tau_{V,\text{em/weak}}^{(\alpha^2)} = 2 \left(\Delta q_V^{(\alpha)} + \Delta r_{\text{fr}}^{(\alpha)} \right) \Delta r_{\text{ferm}}^{(\alpha)} + 2 \Delta r_{\text{fr},2}^{(\alpha^2)}. \quad (45)$$

Note that the factor 2 in these formulae arises due to fact that Δq enters linearly into the muon decay width, see eq. (1), while there is a quadratic dependence on Δr , see eq. (2). The

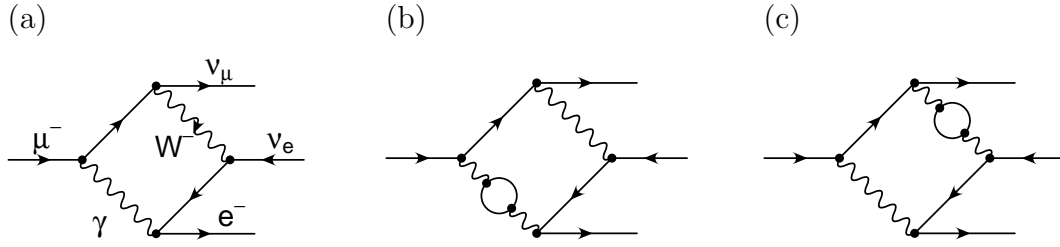


Figure 4: Examples for virtual IR-divergent diagrams contributing to muon decay in the Standard Model. Besides the one-loop diagram (a), at two-loop order, there are diagrams with four (b) and two (c) electromagnetic couplings.

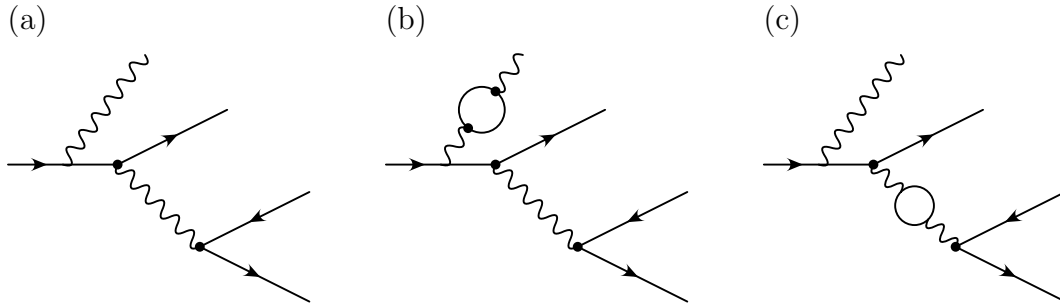


Figure 5: Examples for real bremsstrahlung diagrams in the two-loop calculation of muon decay in the Standard Model, involving one-loop diagrams (a) and two-loop diagrams with four (b) and two (c) QED couplings.

finite remainders are then combined with all remaining virtual Standard Model contributions into $\Delta r^{(\alpha)}$, $\Delta r^{(\alpha^2)}$. In eq. (45) $\Delta r_{\text{ferm}}^{(\alpha)}$ corresponds to the non-QED one-loop corrections with a closed fermion loop.

Besides box-type diagrams, IR divergences are also present in the field renormalisation of the external leptons. Here the correspondence to the Fermi Model contributions is trivial.

Similar to the virtual diagrams, the real bremsstrahlung corrections to muon decay in the Standard Model can be divided into the one-loop contribution $\tau_{\text{R}}^{(\alpha)}$, two-loop corrections with additional electromagnetic couplings only, $\tau_{\text{R,em}}^{(\alpha^2)}$, and mixed QED/non-QED couplings, $\tau_{\text{R,em/weak}}^{(\alpha^2)}$, see Fig. 5. Exploiting the fact that the momentum transfer q^2 through the W boson propagator of these diagrams is much smaller than the W mass, $q^2 \ll M_{\text{W}}^2$, in the limit of zero momentum transfer the real contributions can be reduced to the real Fermi Model contributions,

$$\Delta \tau_{\text{R}}^{(\alpha)} = \Delta q_{\text{R}}^{(\alpha)} \quad (46)$$

$$\Delta \tau_{\text{R,em}}^{(\alpha^2)} = \Delta q_{\text{R}}^{(\alpha^2)} \quad (47)$$

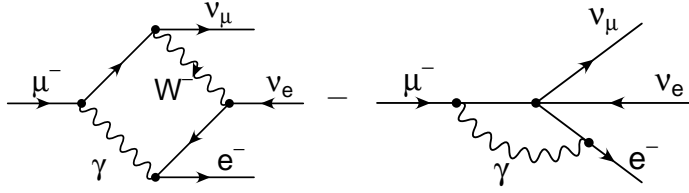


Figure 6: In order to extract the QED corrections already present in the Fermi Model from the Standard Model computation of Δr , differences between QED loop diagrams in the Standard Model and Fermi Model of the same order have to be evaluated, here exemplified for the one-loop case.

$$\Delta\mathcal{T}_{\text{R,em/weak}}^{(\alpha^2)} = 2 \Delta q_{\text{R}}^{(\alpha)} \Delta r_{\text{ferm}}^{(\alpha)}. \quad (48)$$

In total, the contributions to the two-loop Standard Model matrix element amount to

$$\begin{aligned} |\mathcal{M}_{\text{SM}}|^2 &= |\mathcal{M}_{\text{Born}}|^2 \left[\left(1 + \Delta r^{(\alpha)} + \Delta r^{(\alpha^2)}\right)^2 + \Delta q_{\text{V}}^{(\alpha)} + \Delta q_{\text{V}}^{(\alpha^2)} + 2 \Delta q_{\text{V}}^{(\alpha)} \Delta r_{\text{ferm}}^{(\alpha)} \right. \\ &\quad \left. + \Delta q_{\text{R}}^{(\alpha)} + \Delta q_{\text{R}}^{(\alpha^2)} + 2 \Delta q_{\text{R}}^{(\alpha)} \Delta r_{\text{ferm}}^{(\alpha)} \right] \quad (49) \\ &= |\mathcal{M}_{\text{Born}}|^2 \left[(1 + \Delta q)(1 + \Delta r)^2 + \mathcal{O}(\alpha^3) \right], \end{aligned}$$

which can be written in the factorised form at least up to two-loop order including one closed fermion loop. Contributions with two closed fermion loops at $\mathcal{O}(\alpha^2)$ are not present in the Fermi Model and do not contain any IR divergences. Comparing eq. (49) with eq. (42) one obtains

$$|\mathcal{M}_{\text{SM}}|^2 = |\mathcal{M}_{\text{Fermi}}|^2 (1 + \Delta r)^2, \quad (50)$$

showing that a factorisation of electromagnetic corrections to the Fermi Model and the remaining electroweak corrections in the Standard Model according to eq. (1), (2) is possible at least up to the given order.

The calculation of the remaining terms Δr_{fr} , in which the QED Standard Model and Fermi Model contributions in eq. (43)–(45) differ, requires the subtraction of Fermi Model diagrams from Standard Model graphs, as shown in Fig. 6. These terms are IR-finite but UV-divergent and therefore require regularisation. In our approach, dimensional regularisation turns out to be problematic for this purpose since for the computation of the fermion lines in diagrams like those in Fig. 6 we use the Chisholm identity

$$\gamma_{\mu}\gamma_{\nu}\gamma_{\rho} = -i\epsilon_{\mu\nu\rho\sigma}\gamma^{\sigma}\gamma_5 + g_{\mu\nu}\gamma_{\rho} + g_{\nu\rho}\gamma_{\mu} - g_{\mu\rho}\gamma_{\nu}. \quad (51)$$

This identity, however, is only valid in 4 dimensions. In order to circumvent this problem we employ Pauli-Villars regularisation for the QED corrections to the Fermi vertex. The combination of these vertex corrections, Fig. 3 (a), with the QED part of the field renormalisation of the external leptons forms an UV-finite quantity. It is therefore possible to evaluate this combination using Pauli-Villars regularisation (PaVi) and employ dimensional

regularisation (DReg) for the rest. This can formally be written as

$$\begin{aligned} \Delta r_{\text{fr}} = & [\text{QED box graphs in SM}]_{\text{DReg}} - [\text{QED vertex corr. to FM}]_{\text{PaVi}} \\ & + \left[\frac{1}{2} \delta Z_{\text{em}}^{\mu\text{L}} + \frac{1}{2} \delta Z_{\text{em}}^{e\text{L}} \right]_{\text{DReg}} - \left[\frac{1}{2} \delta Z_{\text{em}}^{\mu\text{L}} + \frac{1}{2} \delta Z_{\text{em}}^{e\text{L}} \right]_{\text{PaVi}}. \end{aligned} \quad (52)$$

The index "em" at the field renormalisation constants $\delta Z_{\text{em}}^{\mu\text{L}}$, $\delta Z_{\text{em}}^{e\text{L}}$ indicates that only the QED-like diagrams of the lepton self-energies are taken into account for the calculation of these constants. Since the Standard Model box diagrams are UV finite, they can also be computed with a Pauli-Villars regulator. Thus the cancellation of the IR divergences between the two terms in the first line of eq. (52) proceeds in a straightforward manner and no IR regulator is required.

A similar cancellation of IR divergences takes place for the terms in the second line of eq. (52). This can be made explicit by introducing the Pauli-Villars regulator Λ in photon propagators according to the replacement

$$\frac{1}{k^2} \rightarrow \frac{1}{k^2} - \frac{1}{k^2 - \Lambda^2} \quad (53)$$

with k being the photon momentum. In the difference in the second line of eq. (52) this corresponds to the replacement of the photon propagator in the lepton self-energies by

$$\frac{1}{k^2} \rightarrow \frac{1}{k^2} - \left(\frac{1}{k^2} - \frac{1}{k^2 - \Lambda^2} \right) = \frac{1}{k^2 - \Lambda^2}, \quad (54)$$

or, for the case of two photon propagators in the loop,

$$\begin{aligned} \frac{1}{k^2} \times \frac{1}{k^2} & \rightarrow \frac{1}{k^2} \times \frac{1}{k^2} - \left(\frac{1}{k^2} - \frac{1}{k^2 - \Lambda^2} \right) \times \left(\frac{1}{k^2} - \frac{1}{k^2 - \Lambda^2} \right) \\ & = 2 \frac{1}{k^2} \times \frac{1}{k^2 - \Lambda^2} - \frac{1}{k^2 - \Lambda^2} \times \frac{1}{k^2 - \Lambda^2}. \end{aligned} \quad (55)$$

It can be seen that this replacement effectively leads to the introduction of massive photons with mass Λ so that no IR divergences are present anymore.

5 Numerical Results

We shall now discuss the numerical evaluation of our result for Δr . It should be noted that our definition of Δr according to eq. (2) is based on the expanded form $(1 + \Delta r)$ with $\Delta r = \Delta r^{(\alpha)} + \Delta r^{(\alpha^2)} + \dots$ rather than on the resummed form $1/(1 - \Delta r)$. The terms obtained at two-loop order from a resummation of leading one-loop contributions are directly contained in our two-loop contribution to Δr . The following contributions to Δr are taken into account

$$\Delta r = \Delta r^{(\alpha)} + \Delta r^{(\alpha\alpha_s)} + \Delta r^{(\alpha\alpha_s^2)} + \Delta r^{(N_f\alpha^2)} + \Delta r^{(N_f^2\alpha^2)}, \quad (56)$$

where $\Delta r^{(\alpha)}$ is the one-loop result, eq. (3), $\Delta r^{(\alpha\alpha_s)}$ and $\Delta r^{(\alpha\alpha_s^2)}$ are the two-loop [14] and three-loop [15] QCD corrections, while $\Delta r^{(N_f\alpha^2)}$ is the new electroweak two-loop result.

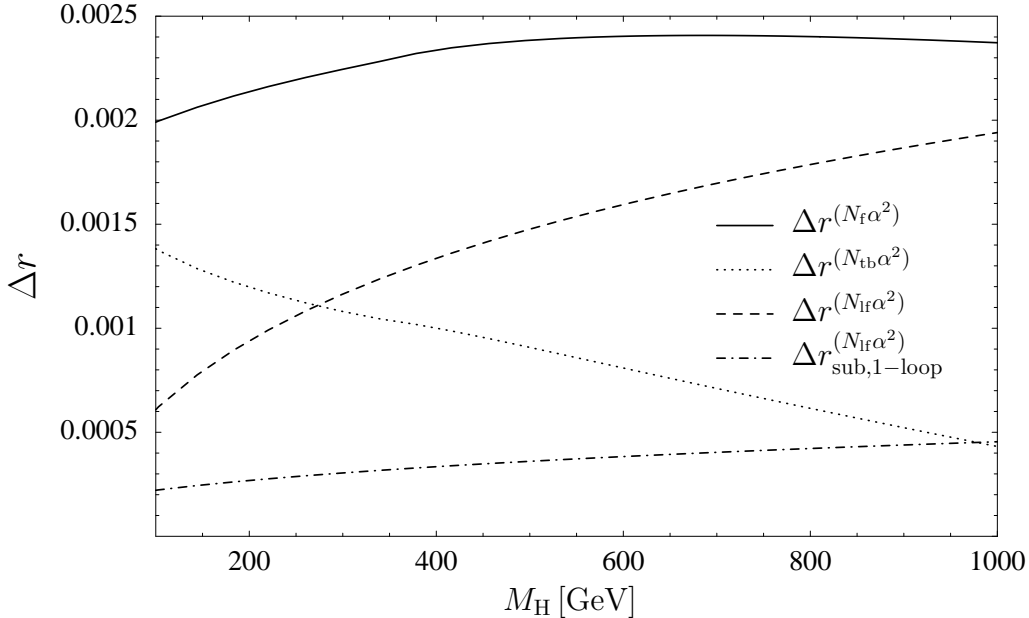


Figure 7: Two-loop contributions with one closed fermion loop to Δr as a function of the Higgs mass. The plot shows the full result, $\Delta r^{(N_f \alpha^2)}$, the contributions from the top-bottom doublet, $\Delta r^{(N_{tb} \alpha^2)}$, and the light-fermion doublets, $\Delta r^{(N_{lf} \alpha^2)}$, as well as the light-fermionic contribution with subtracted resummed terms proportional to $\Delta \alpha$, $\Delta r_{\text{sub},1\text{-loop}}^{(N_{lf} \alpha^2)}$, see eq. (58).

The symbolic notation $(N_f \alpha^2)$ encompasses the contribution of all diagrams containing one fermion loop, i. e. both the top/bottom and light-fermion contributions. Correspondingly, the term $\Delta r^{(N_f^2 \alpha^2)}$ contains the pure fermion-loop contributions in two-loop order.

The pure fermion-loop contributions in three- and four-loop order turn out to be numerically small, as a consequence of accidental numerical cancellations, with a net effect of only about 1 MeV in M_W (using the real-pole definition of the gauge-boson masses) [12]. Furthermore, also the leading three-loop contributions for a large top-quark mass in the limit of zero Higgs mass, proportional to $\alpha^3 m_t^6$ and $\alpha^2 \alpha_s m_t^4$, have very little impact on the prediction of M_W [13]. Therefore these two corrections have not been included in this analysis.

In Figure 7 and Table 1 numerical values for different two-loop contributions with one closed fermion are given as a function of the Higgs boson mass M_H , using $M_W = 80.451$ [5], $m_t = 174.3$ [44] and $\Delta \alpha = 0.05911$ [45]. The contributions with two closed fermion loops are not given in the figure and table since they are independent of M_H . Numerically, they yield a contribution of $\Delta r^{(N_f^2 \alpha^2)} = 16.3 \cdot 10^{-4}$. The Higgs-mass dependence of the two-loop result for Δr agrees perfectly with the result previously obtained in Ref. [21].

It can be seen that both corrections with a top-/bottom-loop, $\Delta r^{(N_{tb} \alpha^2)}$, and with a light-fermion loop, $\Delta r^{(N_{lf} \alpha^2)}$ yield important contributions. At first glance it looks surprising that the light-fermion contributions even dominate over the top-/bottom-contributions for large Higgs masses ($M_H \gtrsim 300$ GeV), which seems to endanger the validity of the large- m_t

M_{H}/GeV	$\Delta r^{(N_{\text{f}}\alpha^2)}/10^{-4}$	$\Delta r^{(N_{\text{tb}}\alpha^2)}/10^{-4}$	$\Delta r^{(N_{\text{lf}}\alpha^2)} - 2\Delta\alpha\Delta r_{\text{bos}}^{(\alpha)}/10^{-4}$
65	20.1	15.7	2.0
100	20.8	14.7	2.2
300	23.3	11.7	3.1
600	24.9	8.9	3.9
1000	24.5	5.1	4.6

Table 1: Two-loop contributions with one closed fermion loop to Δr for different values of the Higgs mass. Besides the full result, $\Delta r^{(N_{\text{f}}\alpha^2)}$, also the contributions from the top-bottom doublet, $\Delta r^{(N_{\text{tb}}\alpha^2)}$, and the light-fermion doublets, $\Delta r^{(N_{\text{lf}}\alpha^2)}$, are given. From the latter the term proportional to $\Delta\alpha$ originating from the resummation prescription eq. (57) is subtracted.

expansions [18, 19, 20]. However, in previous analyses, resummation prescriptions [11] have been derived in order to obtain partial terms of the two-loop result. With the replacement

$$1 + \Delta r \rightarrow \frac{1}{1 - \Delta r} \quad (57)$$

the term $2\Delta\alpha\Delta r_{\text{bos}}^{(\alpha)}$, generated from the charge renormalisation in bosonic one-loop terms, is correctly predicted [11], as we have checked by comparing with the full result, $\Delta r^{(N_{\text{f}}\alpha^2)}$. Therefore, in order to demonstrate the effect of the new two-loop contribution, the difference

$$\Delta r_{\text{sub},1\text{-loop}}^{(N_{\text{lf}}\alpha^2)} = \Delta r^{(N_{\text{lf}}\alpha^2)} - 2\Delta\alpha\Delta r_{\text{bos}}^{(\alpha)} \quad (58)$$

is shown in Figure 7 and Table 1. This expression does not exceed the top-/bottom contributions for any value of the Higgs mass below 1 TeV. The new contribution to Δr from diagrams with a light-fermion loop amounts up to $3.3 \cdot 10^{-4}$ which corresponds to a shift in M_{W} of > 5 MeV.

The prediction for M_{W} is obtained from eq. (2) by means of an iterative procedure, since Δr itself depends on M_{W} ,

$$M_{\text{W}}^2 = M_{\text{Z}}^2 \left\{ \frac{1}{2} + \sqrt{\frac{1}{4} - \frac{\pi\alpha}{\sqrt{2}G_{\mu}M_{\text{Z}}^2} [1 + \Delta r(M_{\text{W}}, M_{\text{Z}}, M_{\text{H}}, m_{\text{t}}, \dots)]} \right\}. \quad (59)$$

In Fig. 8 the prediction for M_{W} based on the results of eq. (56) is shown as a function of M_{H} for $m_{\text{t}} = 174.3 \pm 5.1$ GeV [44] and $\Delta\alpha = 0.05911 \pm 0.00036$ [45]. For comparison, the present experimental value, $M_{\text{W}}^{\text{exp}} = 80.451 \pm 0.033$ GeV [5], and the experimental 95% C.L. lower bound on M_{H} ($M_{\text{H}} = 114.1$ GeV [46]) from the direct search are also indicated. The plot exhibits the well-known preference for a light Higgs boson within the SM. In particular, the theoretical prediction (including the band from a variation of m_{t} , which at present dominates

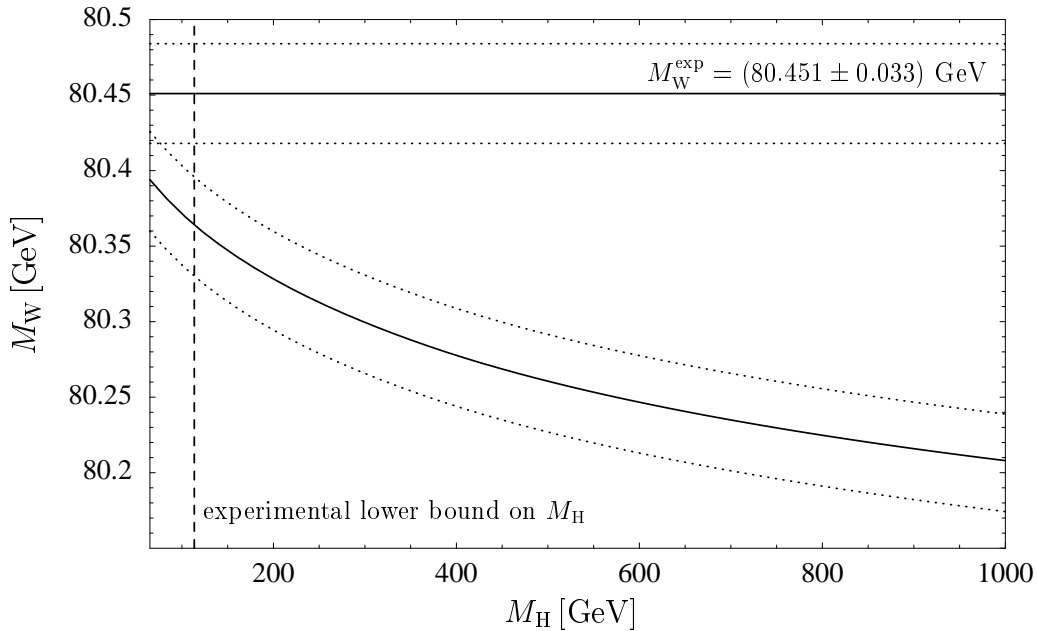


Figure 8: The SM prediction for M_W as a function of M_H for $m_t = 174.3 \pm 5.1$ GeV is compared with the current experimental value, $M_W^{\text{exp}} = 80.451 \pm 0.033$ GeV [5], and the experimental 95% C.L. lower bound on the Higgs-boson mass, $M_H = 114.1$ GeV [46].

the uncertainty of the prediction, see below, and $\Delta\alpha$ within 1σ) cannot be matched with the 1σ region of M_W^{exp} and the 95% C.L. exclusion limit on M_H .

We have compared our results with those of an expansion for asymptotically large values of m_t up to $\mathcal{O}(G_\mu^2 m_t^2 M_Z^2)$ [20, 47]. The results are shown in Table 2 for different values of M_H . The values for the input parameters are taken from Ref. [20], i.e. $m_t = 175$ GeV, $M_Z = 91.1863$ GeV, $\Delta\alpha = 0.0594$, $\alpha_s(M_Z) = 0.118$. One observes a relatively good agreement, with maximal deviations in M_W of about 5 MeV.

It should be noted that the deviations in the last column of Table 2 can not be attributed solely to differences in the two-loop fermionic contributions, because the results also differ by a slightly different treatment of higher-order terms that are not yet under control.

In a further analysis, we have aimed at reducing the latter deviations as far as possible in order to focus on the effects from the two-loop top-quark and light-fermion contributions (see also the discussion in Ref. [22]). While the result of Ref. [20] contains a term $(\Delta r_{\text{bos}}^{(\alpha)})^2$ generated from the purely bosonic one-loop contributions by the resummation eq. (57), no such term is included in our result. A second possible source of deviation could be caused by different implementations of the QCD corrections. We have therefore performed a comparison in which the QCD corrections were removed from both results. With these modifications the maximum deviation between the results is not decreased, see second column in Table 3, but the maximal difference in the Higgs-mass dependence $M_W(M_H) - M_W(M_H = 65 \text{ GeV})$

M_H/GeV	M_W/GeV	$M_W^{\text{expa}}/\text{GeV}$	$\Delta M_W/\text{MeV}$
65	80.3985	80.4039	-5.4
100	80.3759	80.3805	-4.6
300	80.3039	80.3061	-2.2
600	80.2509	80.2521	-1.2
1000	80.2122	80.2129	-0.7

Table 2: The two-loop result for M_W based on eq. (56) is compared with the results of an expansion in m_t up to $\mathcal{O}(G_\mu^2 m_t^2 M_Z^2)$ [20,47], M_W^{expa} . The last column indicates the difference between the two results.

M_H/GeV	$\Delta M'_W/\text{MeV}$	$\Delta M''_W/\text{MeV}$
65	-5.4	-2.3
100	-4.9	-1.6
300	-4.0	0.0
600	-4.3	0.5
1000	-5.0	0.5

Table 3: Investigation of different sources of deviations between the two-loop result for M_W based on eq. (56) and the results of [20,47], M_W^{expa} . In the second column ($\Delta M'_W$), differences in the QCD implementation and in the resummation of bosonic one-loop terms have been eliminated. In the third column ($\Delta M''_W$), in addition the two-loop contributions from light fermions are excluded.

is reduced from 4.7 MeV in Table 2 to 1.4 MeV.

It is also interesting to separately examine the effects of the top-bottom contributions that are not contained in Ref. [20] and of the two-loop terms from the remaining light-fermionic flavours. In the third column in Table 3 we have therefore excluded all light-fermionic $\mathcal{O}(\alpha^2)$ contributions from the comparison. This is achieved by subtracting the expression $\Delta r^{(N_{\text{lf}}\alpha^2)} - 2\Delta r_{\text{lf}}^{(\alpha)} \Delta r_{\text{bos}}^{(\alpha)}$, where the second term $2\Delta r_{\text{lf}}^{(\alpha)} \Delta r_{\text{bos}}^{(\alpha)}$ accounts for the light-fermionic terms that were included in Ref. [20] by means of the resummation prescription eq. (57). The remaining deviations between the results, which now only contain top-/bottom contributions at the two-loop level, are somewhat smaller, while there are larger differences in the Higgs mass dependence of up to 2.8 MeV.

In Ref. [1] a simple formula was given which parametrises our full result for M_W ,

$$M_W = M_W^0 - c_1 dH - c_5 dH^2 + c_6 dH^4 - c_2 d\alpha + c_3 dt - c_7 dH dt - c_4 d\alpha_s, \quad (60)$$

where

$$dH = \ln\left(\frac{M_H}{100 \text{ GeV}}\right), \quad dt = \left(\frac{m_t}{174.3 \text{ GeV}}\right)^2 - 1, \quad d\alpha = \frac{\Delta\alpha}{0.05924} - 1, \quad d\alpha_s = \frac{\alpha_s(M_Z)}{0.119} - 1, \quad (61)$$

and $M_Z = 91.1875 \text{ GeV}$ [5] has been used. By a least square fit we have obtained for the coefficients c_1, \dots, c_7

$$\begin{aligned} M_W^0 &= 80.3755 \text{ GeV}, & c_4 &= 0.0763 \text{ GeV}, \\ c_1 &= 0.0561 \text{ GeV}, & c_5 &= 0.00936 \text{ GeV}, \\ c_2 &= 1.081 \text{ GeV}, & c_6 &= 0.000546 \text{ GeV}, \\ c_3 &= 0.5235 \text{ GeV}, & c_7 &= 0.00573 \text{ GeV}. \end{aligned} \quad (62)$$

The parametrisation of eq. (60) approximates our full result for M_W within 0.4 MeV for $65 \text{ GeV} \leq M_H \leq 1 \text{ TeV}$ and the other input values within their 1σ experimental bounds.

Since this region of validity is in general not sufficient for global fits of the Standard Model, here we supply a more elaborate parametrisation, including the dependence on the Z-boson mass,

$$M_W = M_W^0 - d_1 dH - d_2 dH^2 + d_3 dH^4 - d_4 d\alpha + d_5 dt - d_6 dt^2 - d_7 dH dt - d_8 d\alpha_s + d_9 dZ, \quad (63)$$

with $dZ = M_Z/(91.1875 \text{ GeV}) - 1$ and the other symbols as given in eq. (61). With the following values for the coefficients d_1, \dots, d_9 ,

$$\begin{aligned} M_W^0 &= 80.3756 \text{ GeV}, & d_5 &= 0.5236 \text{ GeV}, \\ d_1 &= 0.05619 \text{ GeV}, & d_6 &= 0.0727 \text{ GeV}, \\ d_2 &= 0.009305 \text{ GeV}, & d_7 &= 0.00544 \text{ GeV}, \\ d_3 &= 0.0005365 \text{ GeV}, & d_8 &= 0.0765 \text{ GeV}, \\ d_4 &= 1.078 \text{ GeV}, & d_9 &= 115.0 \text{ GeV}, \end{aligned} \quad (64)$$

the full result for M_W is approximated by eq. (63) better than 0.3 MeV for $65 \text{ GeV} \leq M_H \leq 1 \text{ TeV}$ and 2σ variations of all other experimental input values.

6 Remaining theoretical uncertainties

Presently, the prediction of the W mass from Δr is mainly affected by the experimental error in the top mass determination, $m_t = 174.3 \pm 5.1$ [44]. This induces an error of $\sim 30 \text{ MeV}$ in the predicted W mass. It is expected that the LHC can reduce the error on the top mass down to about 1.5 GeV [48] and a high-luminosity linear collider even to below 200 MeV [8], resulting in an error in the M_W -prediction from the m_t -uncertainty of $\sim 10 \text{ MeV}$ and $\sim 1.2 \text{ MeV}$, respectively. Another important source of uncertainty is the experimental error in the

determination of $\Delta\alpha$, which in a recent analysis was quoted to be $36 \cdot 10^{-5}$ [45], inducing an error of ~ 6.5 MeV in the predicted W mass. It is expected that this uncertainty will be further reduced significantly in the future [49]. On the other hand, the experimental error of the direct measurement of the W mass, currently 33 MeV, is expected to reduce to 15 MeV for the LHC [7] and 6 MeV for a linear collider running at the W pair threshold [8].

Concerning the theoretical prediction, there are three main sources for uncertainties induced by unknown higher orders: the missing purely bosonic two-loop contributions, three-loop electroweak contributions and the lowest missing QCD corrections of order $\mathcal{O}(\alpha^2\alpha_s)$ and $\mathcal{O}(\alpha\alpha_s^3)$.

For the three-loop $\mathcal{O}(\alpha^3)$ electroweak corrections, partial results are available. In particular the contribution from purely fermionic loops [12] is known, which amounts to a net effect of about 1 MeV in M_W . Recently, the leading terms for large top masses proportional to m_t^6 [13], which enter via the quantity $\Delta\rho$, have been calculated, having an effect of much less than 1 MeV on M_W . However, for the case of the $\mathcal{O}(\alpha^2)$ correction it turned out that the formally leading term $\propto m_t^4$ [19] in the limit $M_H = 0$ is suppressed relative to the next term $\propto m_t^2$ [20], which suggests that the full $\mathcal{O}(\alpha^3)$ corrections could be of $\mathcal{O}(1$ MeV). Alternatively, one could try to estimate their size from residual scheme dependencies of the $\mathcal{O}(\alpha^2)$ result. For example, the W width is needed at tree-level in order to translate between the different Breit-Wigner parametrisations mentioned in section 3.2. Whether Γ_W is parametrised with α or G_μ is formally of order $\mathcal{O}(\alpha^3)$ and also results in a shift in M_W of $\mathcal{O}(1$ MeV).

For the QCD correction of order $\mathcal{O}(\alpha^2\alpha_s)$, the leading contribution $\propto m_t^4$ in an expansion for large m_t has been calculated in the limit of vanishing Higgs mass [13]. It turned out to result in a W mass shift of only less than 0.5 MeV. However, as explained above, the formally leading term $\propto m_t^4$ can be suppressed relative to the sub-leading terms, so that the total $\mathcal{O}(\alpha^2\alpha_s)$ contribution could be considerably larger.

Higher order QCD contributions may be estimated from the renormalisation scale dependence of the available results. For this purpose running $\overline{\text{MS}}$ values at different scales are used for the top-mass m_t or strong coupling α_s . With this variation in the $\mathcal{O}(\alpha^2)$ result we obtain a shift in M_W of ≈ 3.8 MeV, which gives an estimate of the $\mathcal{O}(\alpha^2\alpha_s)$ contributions. Accordingly, from the scale dependence of the $\mathcal{O}(\alpha\alpha_s^2)$ result, we estimate the effect of the $\mathcal{O}(\alpha\alpha_s^3)$ term to yield ≈ 0.7 MeV.

A second method for estimating the missing QCD corrections relies on the assumption that the ratios of consecutive coefficients in the perturbative series do not change very much. In this case the ratio between the $\mathcal{O}(\alpha^2\alpha_s)$ and $\mathcal{O}(\alpha^2)$ contributions to Δr should be of the same size as the ratio between $\Delta r^{(\alpha\alpha_s)}$ and $\Delta r^{(\alpha)}$ ³. From this we deduce that the effect of the $\mathcal{O}(\alpha^2\alpha_s)$ contribution on M_W is about 3.5 MeV, which is in nice agreement with the previous estimate. In a similar manner, we can compare the ratios $\Delta r^{(\alpha\alpha_s^2)}/\Delta r^{(\alpha\alpha_s)}$ and $\Delta r^{(\alpha\alpha_s^3)}/\Delta r^{(\alpha\alpha_s^2)}$ and obtain ≈ 0.7 MeV for the impact of the $\mathcal{O}(\alpha\alpha_s^3)$ contribution.

The third important higher order contribution, the bosonic $\mathcal{O}(\alpha^2)$ correction, is more difficult to estimate. In a simple approach the one-loop bosonic contribution is resummed

³This ratio amounts to $\approx 12\%$ in accordance with $\alpha_s(M_Z)$.

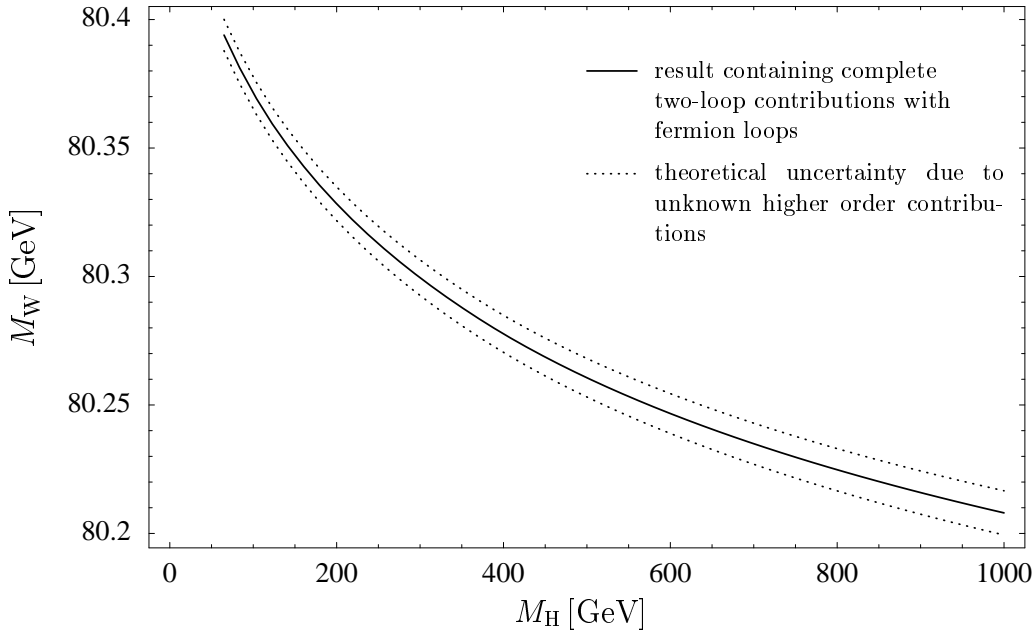


Figure 9: Theoretical error band of the M_W -prediction due to unknown higher order contributions.

according to the prescription eq. (57) which results in a term $(\Delta r_{\text{bos}}^{(\alpha)})^2$. This term shifts the W mass by less than 0.5 MeV for $M_H = 100$ GeV, but more than 2.5 MeV for $M_H = 1$ TeV.

We obtain the total theory uncertainty by linearly adding up all sources for theoretical errors. This results in an uncertainty for M_W of 6 MeV for light Higgs masses and about 8 MeV for $M_H \sim 1$ TeV, which is similar to the value given in Ref. [50]. The error band due to these theoretical uncertainties is shown in Figure 9.

Recently the new two-loop results for the prediction of the W-boson mass have been implemented into the Standard Model fits with ZFITTER [51] and are subject to the latest LEP electroweak analyses [5]. While the effect on the predicted value for M_W is relatively small compared to the experimental error, it induces a significant shift in the prediction of the effective leptonic weak mixing angle $\sin^2 \theta_{\text{eff}}^{\text{lept}}$ according to

$$\sin^2 \theta_{\text{eff}}^{\text{lept}} = \left(1 - \frac{M_W^2}{M_Z^2}\right) \kappa(M_W^2), \quad (65)$$

where κ incorporates the contributions from radiative corrections. The effect of inserting the new result for M_W in eq. (65) instead of the previous result obtained from an expansion in powers of m_t [20] amounts to an upward shift of about $8 \cdot 10^{-5}$, which is about half the experimental error of $17 \cdot 10^{-5}$ [5]. Since the corresponding complete fermionic two-loop corrections for κ are not yet known, this shift has been treated as a theoretical uncertainty and is represented as a rather wide band in the well-known *blue-band plot* [5].

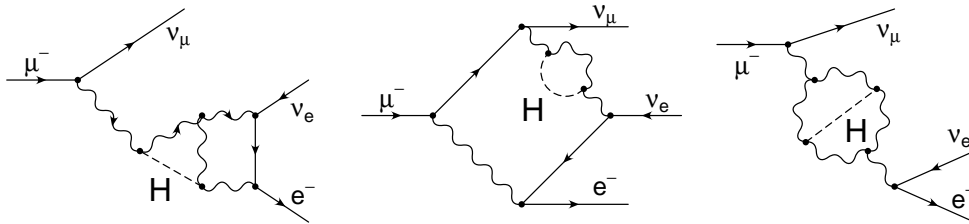


Figure 10: Examples for types of bosonic two-loop diagrams with internal Higgs bosons contributing to muon decay.

7 Higgs-mass dependence of bosonic two-loop result

As a first step towards a full $\mathcal{O}(\alpha^2)$ result for Δr we have calculated the dependence of the bosonic two-loop corrections on the Higgs-boson mass. This includes the evaluation of all diagrams without closed fermion loops which contain internal Higgs bosons or M_H -dependent scalar couplings. Some typical examples are given in Figure 10. This subset of the complete bosonic two-loop corrections can be evaluated with the methods described in sections 2–4. In particular, the factorisation of IR-divergent QED corrections as in eq. (49) also applies for the bosonic M_H -dependent contributions.

In order to study the Higgs-mass dependence, the subtracted quantity

$$\Delta r_{\text{bos,sub}}^{(\alpha^2)}(M_H, M_H^0) = \Delta r_{\text{bos}}^{(\alpha^2)}(M_H) - \Delta r_{\text{bos}}^{(\alpha^2)}(M_H^0) \quad (66)$$

is considered, using a fixed offset value for the Higgs-boson mass, $M_H^0 = 100$ GeV. The contribution of the M_H -dependent diagrams to $\Delta r_{\text{bos,sub}}^{(\alpha^2)}(M_H, M_H^0)$ forms a finite and gauge-parameter independent quantity, as we have explicitly checked. This analysis is in analogy to Ref. [21], where the corresponding quantity for the fermionic two-loop contributions was studied.

In Table 4 the variation of the prediction for the W-mass M_W as a function of the Higgs mass M_H is shown without and with the bosonic two-loop terms, using the input values of Table 1. As before the values are given in terms of the subtracted quantity

$$M_{W,\text{sub}}(M_H) = M_W(M_H) - M_W(M_H^0 = 100 \text{ GeV}). \quad (67)$$

Figure 11 shows how the slope of the Higgs-mass dependence is modified due to the inclusion of the bosonic two-loop terms. The maximum change amounts to less than 2 MeV in the region $100 \text{ GeV} < M_H < 1 \text{ TeV}$. As a consequence, from the M_H -dependence we get no indications for any particularly large effects in the full bosonic two-loop corrections to Δr . In this context we would like to point out the observation that the Higgs-mass dependence of the fermionic two-loop corrections [21] provides a rough assessment of the effect of the full two-loop corrections [1]. This supports the estimation in section 6 that the expected size of the purely bosonic $\mathcal{O}(\alpha^2)$ contributions is relatively small.

M_H / GeV	$M_{W,\text{sub}}^{\text{ferm}} / \text{MeV}$	$M_{W,\text{sub}}^{\text{ferm}+\text{bos}} / \text{MeV}$	$\Delta M_{W,\text{sub}} / \text{MeV}$
100	0	0	0
200	-43.1	-42.6	0.5
400	-93.7	-93.0	0.8
600	-124.7	-123.8	1.0
1000	-163.4	-161.7	1.7

Table 4: Shift in the predicted W mass caused by varying Higgs-boson mass M_H when including fermionic two-loop corrections ($M_{W,\text{sub}}^{\text{ferm}}$) and all two-loop corrections ($M_{W,\text{sub}}^{\text{ferm}+\text{bos}}$). $\Delta M_{W,\text{sub}}$ gives the difference between these two contributions, i. e. the effect of the bosonic loops.

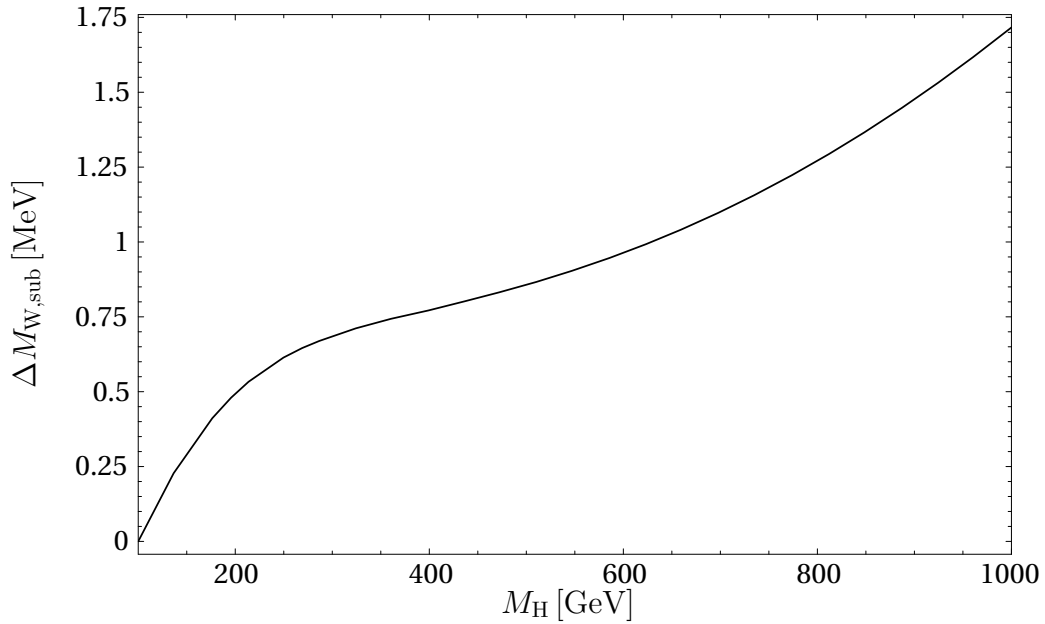


Figure 11: Variation of the Higgs-mass dependence of the M_W -prediction due to the inclusion of bosonic two-loop corrections.

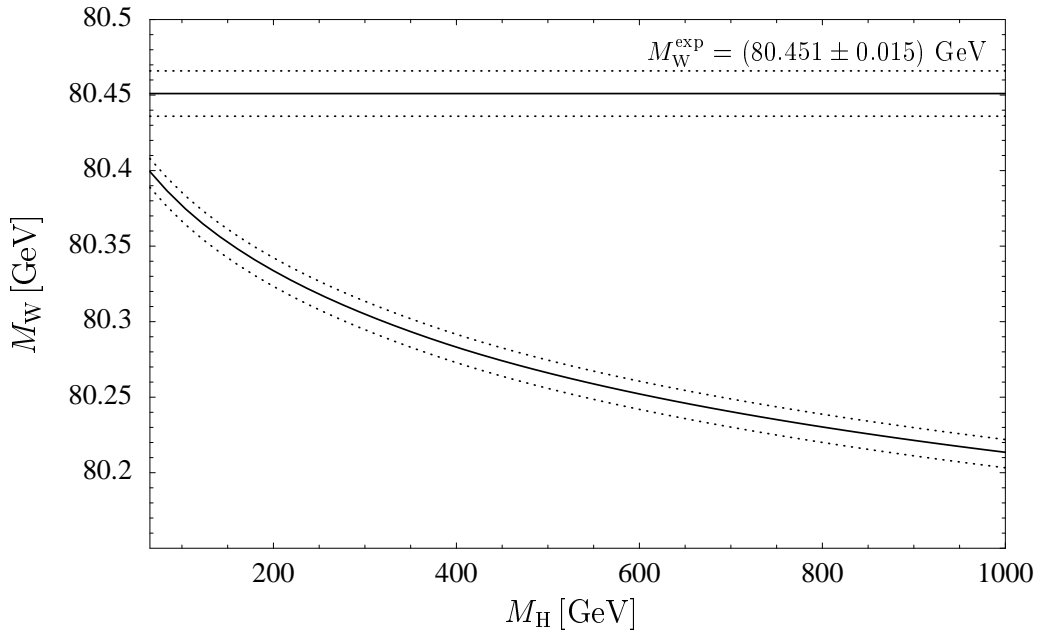


Figure 12: Comparison of prediction and measurement for M_W using expected experimental uncertainties at the LHC and the current central values.

8 Prospects for future colliders

In the following we illustrate the accuracy that can be reached with future colliders concerning tests of electroweak physics. Taking the current central values of the experimental input values, Fig. 12 shows the situation that can be obtained with the LHC with expected errors for M_W and m_t of $\delta M_W = 15$ MeV and $\delta m_t = 1.5$ GeV, respectively. Even more impressive results could be achieved by a high-luminosity linear collider running at low energies, where errors of $\delta M_W = 6$ MeV and $\delta m_t = 200$ MeV may be obtained [8], see Fig. 13. In both figures we furthermore assumed that the error in the shift of the electromagnetic fine structure constant, $\Delta\alpha$, will be cut to half of the present value.

9 Conclusion

In this paper, the evaluation of the complete fermionic two-loop contributions to the M_W – M_Z mass correlation was described, elucidating the applied techniques and the implications of the new result.

The renormalisation within the on-shell scheme was described in detail. In particular, the definition of the gauge-boson masses via the complex pole of the S matrix was studied, ensuring in particular gauge-parameter independence of the renormalised weak mixing angle and the gauge boson masses. The latter requires to take tadpole contributions into account.

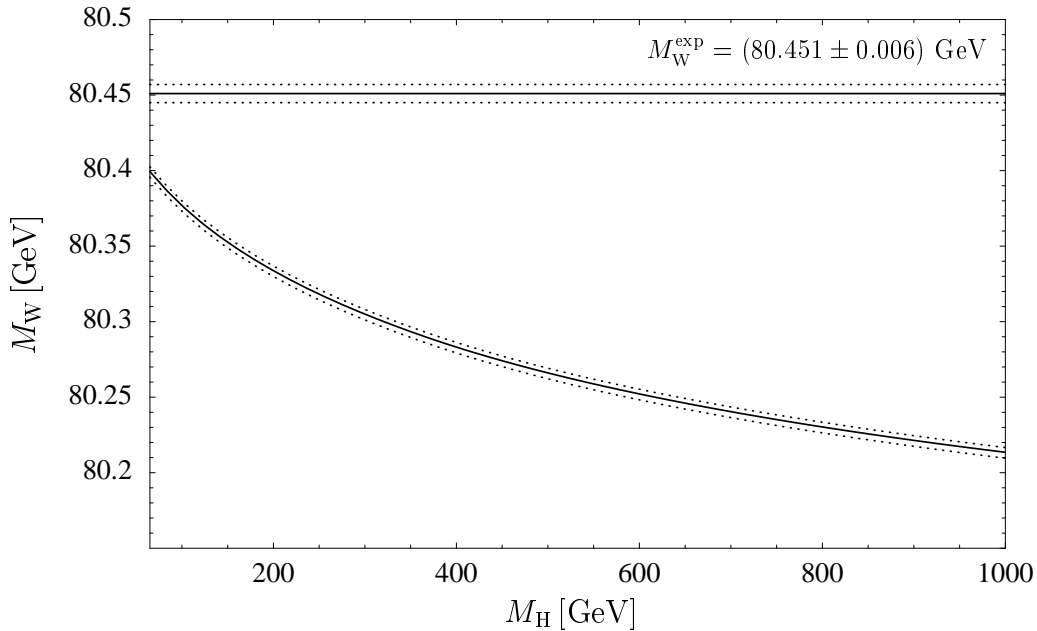


Figure 13: Comparison of prediction and measurement for M_W for expected experimental errors at a high-luminosity linear collider, assuming current central values.

It was shown how the radiative corrections in the Standard Model can be factorised from the QED corrections within the Fermi Model.

The result for M_W was expressed in terms of an accurate numerical parametrisation valid for all values of the Higgs mass up to 1 TeV. A detailed comparison with a previous result obtained by an expansion in powers of m_t up to next-to-leading order was performed. Here the effects of the top/bottom and light-fermion contributions were studied separately and found to yield a contribution of a few MeV to the prediction of M_W each.

Furthermore, the remaining theoretical uncertainties due to unknown higher orders were discussed and an overall uncertainty of the W-boson mass prediction of ~ 6 MeV was estimated for light Higgs-boson masses. A careful treatment of the theoretical uncertainties proved to be important for precision tests of the Standard Model. The situation for present experimental uncertainties was contrasted to the capabilities of aspired future colliders.

As an additional result, the Higgs-mass dependence of the purely bosonic electroweak two-loop contributions was computed, so that the only yet missing piece of the complete two-loop calculation for Δr , i. e. muon decay, is a constant (M_H -independent) contribution. The numerical impact of the bosonic two-loop corrections on the Higgs-mass dependence of the M_W -prediction is relatively small, in accordance with our estimates for theoretical uncertainties.

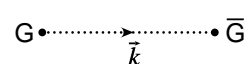
Acknowledgements

We thank D. Bardin, P. Gambino, M. Grünewald, S. Heinemeyer, T. Hurth and G. Quast for useful discussions and communications. We also thank D. Bardin for cooperation in implementing our result in ZFITTER. This work was supported in part by the European Community's Human Potential Programme under contract HPRN-CT-2000-00149 Physics at Colliders.

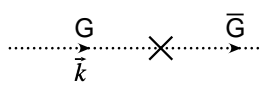
We are grateful to M. Awramik and M. Czakon for detailed comparisons with their results [52], which helped to debug our computation. After correcting our calculation, there is now perfect agreement between both results.

Appendix

In the appendix the explicit Feynman rules for the ghost interactions in the Standard Model are listed. In the vertices all particles are considered as incoming. The following expressions comply with a non-renormalisation of the gauge-fixing sector and the use of a linear R_ξ gauge, introducing the (renormalised) gauge parameters ξ^γ, ξ^Z, ξ^W according to eqs. (23)–(25). Counterterms in the one-loop approximation are included. The Feynman rules for the other sectors of the theory can be found e. g. in Ref. [37].

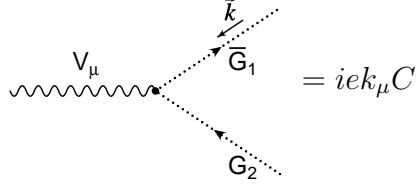
ghost propagator		$= \frac{i (\xi^G)^{\frac{1}{2}}}{k^2 - \xi^G M_G^2}$
------------------	---	---

$$\bar{u}^\gamma u^\gamma : \frac{i (\xi^\gamma)^{\frac{1}{2}}}{k^2} \quad \bar{u}^Z u^Z : \frac{i (\xi^Z)^{\frac{1}{2}}}{k^2 - \xi^Z M_Z^2} \quad \bar{u}^\pm u^\pm : \frac{i (\xi^W)^{\frac{1}{2}}}{k^2 - \xi^W M_W^2} \quad (68)$$

\overline{GG} counterterm		$= i (C_1 k^2 - C_2)$
-----------------------------	---	-----------------------

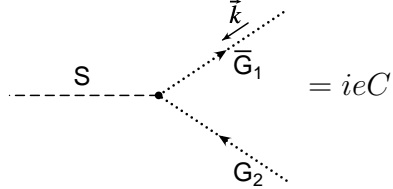
$$\begin{aligned}
 \bar{u}^\gamma u^\gamma : C_1 &= (\xi^\gamma)^{-\frac{1}{2}} \left(1 - \frac{1}{2} \delta Z^{\gamma\gamma} \right) & C_2 &= 0 \\
 \bar{u}^\gamma u^Z : C_1 &= (\xi^\gamma)^{-\frac{1}{2}} \left(-\frac{1}{2} \delta Z^{\gamma Z} \right) & C_2 &= 0 \\
 \bar{u}^Z u^\gamma : C_1 &= (\xi^Z)^{-\frac{1}{2}} \left(-\frac{1}{2} \delta Z^{Z\gamma} \right) & C_2 &= 0 \\
 \bar{u}^Z u^Z : C_1 &= (\xi^Z)^{-\frac{1}{2}} \left(1 - \frac{1}{2} \delta Z^{ZZ} \right) & C_2 &= (\xi^Z)^{\frac{1}{2}} \left(M_Z^2 (1 - \frac{1}{2} \delta Z^X) + \frac{1}{2} \delta M_Z^2 \right) \\
 \bar{u}^\pm u^\pm : C_1 &= (\xi^W)^{-\frac{1}{2}} \left(1 - \frac{1}{2} \delta Z^W \right) & C_2 &= (\xi^W)^{\frac{1}{2}} \left(M_W^2 (1 - \frac{1}{2} \delta Z^\phi) + \frac{1}{2} \delta M_W^2 \right)
 \end{aligned} \quad (69)$$

$\overline{G}_1 G_2 V$ coupling



$$\begin{aligned}
\bar{u}^\pm u^\pm \gamma : C &= \pm (\xi^W)^{-\frac{1}{2}} \left(1 + \delta Z_e + \frac{1}{2} \delta Z^{\gamma\gamma} - \frac{1}{2} \delta Z^W - \frac{c_W}{2s_W} \delta Z^{Z\gamma} \right) \\
\bar{u}^\pm u^\pm Z : C &= \mp \frac{c_W}{s_W} (\xi^W)^{-\frac{1}{2}} \left(1 + \delta Z_e + \frac{1}{2} \delta Z^{ZZ} - \frac{1}{2} \delta Z^W - \frac{\delta s_W}{s_W c_W^2} - \frac{s_W}{2c_W} \delta Z^{\gamma Z} \right) \\
\bar{u}^\gamma u^\mp W^\pm : C &= \pm (\xi^\gamma)^{-\frac{1}{2}} \left(1 + \delta Z_e + \frac{1}{2} \delta Z^W - \frac{1}{2} \delta Z^{\gamma\gamma} \right) \pm \frac{c_W}{2s_W} (\xi^\gamma)^{-\frac{1}{2}} \delta Z^{\gamma Z} \\
\bar{u}^Z u^\mp W^\pm : C &= \mp \frac{c_W}{s_W} (\xi^Z)^{-\frac{1}{2}} \left(1 + \delta Z_e + \frac{1}{2} \delta Z^W - \frac{1}{2} \delta Z^{ZZ} - \frac{\delta s_W}{s_W c_W^2} \right) \mp \frac{1}{2} (\xi^Z)^{-\frac{1}{2}} \delta Z^{\gamma Z} \\
\bar{u}^\pm u^\gamma W^\pm : C &= \mp (\xi^W)^{-\frac{1}{2}} (1 + \delta Z_e) \\
\bar{u}^\pm u^Z W^\pm : C &= \pm \frac{c_W}{s_W} (\xi^W)^{-\frac{1}{2}} \left(1 + \delta Z_e - \frac{\delta s_W}{s_W c_W^2} \right)
\end{aligned} \tag{70}$$

$\overline{G}_1 G_2 S$ coupling



$$\begin{aligned}
\bar{u}^Z u^Z H : C &= -\frac{1}{2s_W c_W} M_Z (\xi^Z)^{\frac{1}{2}} \left(1 + \delta Z_e + \frac{s_W^2 - c_W^2}{c_W^2} \frac{\delta s_W}{s_W} + \frac{1}{2} \delta Z^H - \frac{1}{2} \delta Z^\chi \right) \\
\bar{u}^\pm u^\pm H : C &= -\frac{1}{2s_W} M_W (\xi^W)^{\frac{1}{2}} \left(1 + \delta Z_e - \frac{\delta s_W}{s_W} + \frac{1}{2} \delta Z^H - \frac{1}{2} \delta Z^\phi \right) \\
\bar{u}^\pm u^\pm \chi : C &= \mp i \frac{1}{2s_W} M_W (\xi^W)^{\frac{1}{2}} \left(1 + \delta Z_e - \frac{\delta s_W}{s_W} + \frac{1}{2} \delta Z^\chi - \frac{1}{2} \delta Z^\phi \right) \\
\bar{u}^Z u^\mp \phi^\pm : C &= \frac{1}{2s_W} M_Z (\xi^Z)^{\frac{1}{2}} \left(1 + \delta Z_e - \frac{\delta s_W}{s_W} + \frac{1}{2} \delta Z^\phi - \frac{1}{2} \delta Z^\chi \right) \\
\bar{u}^\pm u^\gamma \phi^\pm : C &= M_W (\xi^W)^{\frac{1}{2}} (1 + \delta Z_e) \\
\bar{u}^\pm u^Z \phi^\pm : C &= \frac{s_W^2 - c_W^2}{2s_W c_W} M_W (\xi^W)^{\frac{1}{2}} \left(1 + \delta Z_e + \frac{1}{(s_W^2 - c_W^2) c_W^2} \frac{\delta s_W}{s_W} \right)
\end{aligned} \tag{71}$$

References

- [1] A. Freitas, W. Hollik, W. Walter and G. Weiglein, Phys. Lett. B **495** (2000) 338 [hep-ph/0007091];
A. Freitas, S. Heinemeyer, W. Hollik, W. Walter and G. Weiglein, Nucl. Phys. Proc. Suppl. **89** (2000) 82 [hep-ph/0007129];
A. Freitas, S. Heinemeyer, W. Hollik, W. Walter and G. Weiglein, hep-ph/0101260, in *Proceedings of the 5th International Symposium on Radiative Corrections* (RADCOR 2000), Carmel, California, September 2000.
- [2] R. E. Behrends, R. J. Finkelstein and A. Sirlin, Phys. Rev. **101** (1956) 866;
S. M. Berman, Phys. Rev. **112** (1958) 267;
T. Kinoshita and A. Sirlin, Phys. Rev. **113** (1959) 1652.
- [3] T. van Ritbergen and R. G. Stuart, Phys. Rev. Lett. **82** (1999) 488 [hep-ph/9808283];
T. van Ritbergen and R. G. Stuart, Nucl. Phys. B **564** (2000) 343 [hep-ph/9904240];
M. Steinhauser and T. Seidensticker, Phys. Lett. B **467** (1999) 271 [hep-ph/9909436].
- [4] A. Sirlin, Phys. Rev. D **22** (1980) 971;
W. J. Marciano and A. Sirlin, Phys. Rev. D **22** (1980) 2695 [Erratum-ibid. D **31** (1980) 213].
- [5] D. Charlton, hep-ex/0110086, in *Proceedings of the Intl. Europhysics Conference on High-Energy Physics* (HEP 2001), Budapest, July 2001;
J. Drees, hep-ex/0110077, in *Proceedings of the XX Intl. Symposium on Lepton and Photon Interactions at High Energies*, Rome, July 2001.
- [6] D. Amidei et al., *Future Electroweak Physics at the Fermilab Tevatron* in *Report of the tev_2000 Study Group* (1996), FERMILAB-PUB-96/082.
- [7] ATLAS Collaboration, “Detector and Physics Performance Technical Design Report”, CERN/LHCC/99-15 (1999);
CMS Collaboration, Technical Design Reports, CMS TDR 1–5 (1997/98);
S. Haywood et al., *Electroweak physics*, hep-ph/0003275, in *Proceedings of the Workshop on Standard Model Physics (and more) at the LHC*, eds. G. Altarelli and M.L. Mangano (Report CERN 2000–004).
- [8] TESLA Technical Design Report, Part III, eds. R. Heuer, D. J. Miller, F. Richard and P. M. Zerwas, DESY-2001-11C, hep-ph/0106315;
T. Abe *et al.* [American Linear Collider Working Group Collaboration], hep-ex/0106057, in *Proc. of the APS/DPF/DPB Summer Study on the Future of Particle Physics (Snowmass 2001)* eds. R. Davidson and C. Quigg.
- [9] S. Heinemeyer, T. Mannel and G. Weiglein, DESY 99-117, hep-ph/9909538, in *Proceedings of the International Workshop on Linear Colliders*, Sitges, April/May 1999;

- J. Erler, S. Heinemeyer, W. Hollik, G. Weiglein and P. M. Zerwas, Phys. Lett. B **486** (2000) 125 [hep-ph/0005024].
- [10] M. J. Veltman, Nucl. Phys. B **123** (1977) 89.
- [11] W. J. Marciano, Phys. Rev. D **20** (1979) 274;
A. Sirlin, Phys. Rev. D **29** (1984) 89;
M. Consoli, W. Hollik and F. Jegerlehner, Phys. Lett. B **227** (1989) 167.
- [12] G. Weiglein, Acta Phys. Polon. B **29** (1998) 2735 [hep-ph/9807222];
A. Stremplatt, Diploma thesis (Univ. of Karlsruhe, 1998).
- [13] J. J. van der Bij, K. G. Chetyrkin, M. Faisst, G. Jikia and T. Seidensticker, Phys. Lett. B **498** (2001) 156 [hep-ph/0011373].
- [14] A. Djouadi and C. Verzegnassi, Phys. Lett. B **195** (1987) 265;
A. Djouadi, Nuovo Cim. A **100** (1988) 357;
B. A. Kniehl, Nucl. Phys. B **347** (1990) 86;
F. Halzen and B. A. Kniehl, Nucl. Phys. B **353** (1991) 567;
B. A. Kniehl and A. Sirlin, Nucl. Phys. B **371** (1992) 141;
B. A. Kniehl and A. Sirlin, Phys. Rev. D **47** (1993) 883;
A. Djouadi and P. Gambino, Phys. Rev. D **49** (1994) 3499 [Erratum-ibid. D **53** (1994) 4111] [hep-ph/9309298].
- [15] L. Avdeev, J. Fleischer, S. Mikhailov and O. Tarasov, Phys. Lett. B **336** (1994) 560 [Erratum-ibid. B **349** (1994) 597] [hep-ph/9406363];
K. G. Chetyrkin, J. H. Kühn and M. Steinhauser, Phys. Lett. B **351** (1995) 331 [hep-ph/9502291];
K. G. Chetyrkin, J. H. Kühn and M. Steinhauser, Phys. Rev. Lett. **75** (1995) 3394 [hep-ph/9504413].
- [16] K. G. Chetyrkin, J. H. Kühn and M. Steinhauser, Nucl. Phys. B **482** (1996) 213 [hep-ph/9606230].
- [17] J. van der Bij and M. J. Veltman, Nucl. Phys. B **231** (1984) 205.
- [18] J. J. van der Bij and F. Hoogeveen, Nucl. Phys. B **283** (1987) 477.
- [19] R. Barbieri, M. Beccaria, P. Ciafaloni, G. Curci and A. Vicere, Phys. Lett. B **288** (1992) 95 [Erratum-ibid. B **312** (1992) 511] [hep-ph/9205238];
R. Barbieri, M. Beccaria, P. Ciafaloni, G. Curci and A. Vicere, Nucl. Phys. B **409** (1993) 105;
J. Fleischer, O. V. Tarasov and F. Jegerlehner, Phys. Lett. B **319** (1993) 249;
J. Fleischer, O. V. Tarasov and F. Jegerlehner, Phys. Rev. D **51** (1995) 3820.
- [20] G. Degrassi, P. Gambino and A. Vicini, Phys. Lett. B **383** (1996) 219 [hep-ph/9603374];
G. Degrassi, P. Gambino and A. Sirlin, Phys. Lett. B **394** (1997) 188 [hep-ph/9611363].

- [21] S. Bauberger and G. Weiglein, Phys. Lett. B **419** (1998) 333 [hep-ph/9707510];
G. Weiglein, hep-ph/9901317, in *Proceedings of the IVth International Symposium on Radiative Corrections*, ed. J. Solà (World Scientific, Singapore, 1999), p. 410.
- [22] P. Gambino, A. Sirlin and G. Weiglein, JHEP **9904** (1999) 025 [hep-ph/9903249].
- [23] F. Jegerlehner, M. Y. Kalmykov and O. Veretin, hep-ph/0105304.
- [24] P. Malde and R. G. Stuart, Nucl. Phys. B **552** (1999) 41 [hep-ph/9903403].
- [25] J. Küblbeck, M. Böhm and A. Denner, Comput. Phys. Commun. **60** (1990) 165;
H. Eck and J. Küblbeck, *Guide to FeynArts1.0* (Univ. of Würzburg, 1992);
T. Hahn, Nucl. Phys. Proc. Suppl. **89** (2000) 231 [hep-ph/0005029];
T. Hahn, *FeynArts2.2 User's Guide* (Univ. of Karlsruhe, 2000)
- [26] G. Weiglein, R. Scharf and M. Böhm, Nucl. Phys. B **416** (1994) 606 [hep-ph/9310358];
G. Weiglein, R. Mertig, R. Scharf and M. Böhm, in *New Computing Techniques in Physics Research 2*, ed. D. Perret-Gallix (World Scientific, Singapore, 1992), p. 617.
- [27] G. 't Hooft and M. J. Veltman, Nucl. Phys. B **153** (1979) 365.
- [28] A. I. Davydychev and J. B. Tausk, Nucl. Phys. B **397** (1993) 123.
- [29] S. Bauberger, F. A. Berends, M. Böhm and M. Buza, Nucl. Phys. B **434** (1995) 383 [hep-ph/9409388];
S. Bauberger, F.A. Berends, M. Böhm, M. Buza and G. Weiglein, Nucl. Phys. Proc. Suppl. **37B** (1994) 95 [hep-ph/9406404];
S. Bauberger and M. Böhm, Nucl. Phys. B **445** (1995) 25 [hep-ph/9501201].
- [30] C. G. Bollini and J. J. Giambiagi, Nuovo Cim. B **12** (1972) 20;
J. F. Ashmore, Lett. Nuovo Cim. **4** (1972) 289.
- [31] G. 't Hooft and M. J. Veltman, Nucl. Phys. B **44** (1972) 189.
- [32] W. A. Bardeen, R. Gastmans and B. Lautrup, Nucl. Phys. B **46** (1972) 319.
- [33] P. Breitenlohner and D. Maison, Commun. Math. Phys. **52** (1977) 11.
- [34] F. Jegerlehner, Eur. Phys. J. C **18** (2001) 673 [hep-th/0005255].
- [35] P. A. Grassi, T. Hurth and M. Steinhauser, Ann.Phys. **288** (2001) 197 [hep-ph/9907426];
P. A. Grassi and T. Hurth, hep-ph/0101183, in *Proceedings of the 5th International Symposium on Radiative Corrections (RADCOR 2000)*, Carmel, California, September 2000.
- [36] M. Jamin and M. E. Lautenbacher, Comput. Phys. Commun. **74** (1993) 265.

- [37] A. Denner, Fortsch. Phys. **41** (1993) 307.
- [38] S. Bauberger and G. Weiglein, Nucl. Instrum. Meth. A**389** (1997) 318 [hep-ph/9611445].
- [39] S. Bauberger, Doctoral thesis (Univ. of Würzburg, 1997).
- [40] S. Willenbrock and G. Valencia, Phys. Lett. B **259** (1991) 373;
 A. Sirlin, Phys. Rev. Lett. **67** (1991) 2127;
 R. G. Stuart, Phys. Lett. B **262** (1991) 113;
 H. Veltman, Z. Phys. C **62** (1994) 35;
 M. Passera and A. Sirlin, Phys. Rev. D **58** (1998) 113010 [hep-ph/9804309];
 P. Gambino and P. A. Grassi, Phys. Rev. D **62** (2000) 076002 [hep-ph/9907254];
 A. R. Bohm and N. L. Harshman, Nucl. Phys. B **581** (2000) 91 [hep-ph/0001206].
- [41] A. Denner, G. Weiglein and S. Dittmaier, Nucl. Phys. B **440** (1995) 95 [hep-ph/9410338].
- [42] D. Y. Bardin, A. Leike, T. Riemann and M. Sachwitz, Phys. Lett. B **206** (1988) 539.
- [43] M.L. Nekrasov, talk presented at the XVth International Workshop *High Energy Physics and Quantum Field Theory*, Tver, September 2000, hep-ph/0102284;
 B. A. Kniehl and A. Sirlin, hep-ph/0110296.
- [44] D. E. Groom *et al.* [Particle Data Group Collaboration], Eur. Phys. J. C **15** (2000) 1.
- [45] H. Burkhardt and B. Pietrzyk, LAPP-EXP-2001-03.
- [46] The LEP working group for Higgs boson searches, LHWG-NOTE-2001-03, hep-ex/0107029.
- [47] P. Gambino, private communication.
- [48] M. Beneke *et al.*, *Top quark physics*, in *Proceedings of the Workshop on Standard Model Physics (and more) at the LHC*, eds. G. Altarelli and M.L. Mangano (Report CERN 2000-004).
- [49] F. Jegerlehner, LC Note LC-TH-2001-035, hep-ph/0105283.
- [50] U. Baur *et al.*, hep-ph/0202001, in *Proc. of the APS/DPF/DPB Summer Study on the Future of Particle Physics (Snowmass 2001)* eds. R. Davidson and C. Quigg.
- [51] D. Y. Bardin, P. Christova, M. Jack, L. Kalinovskaya, A. Olchevski, S. Riemann and T. Riemann, Comput. Phys. Commun. **133** (2001) 229 [hep-ph/9908433].
- [52] M. Awramik and M. Czakon, Phys. Rev. Lett. **89** (2002) 241801 [hep-ph/0208113];
 M. Awramik, M. Czakon, A. Onishchenko and O. Veretin, hep-ph/0209084;
 M. Awramik and M. Czakon, hep-ph/0305248.